Bio-compatible coatings for bone implants

Deborah J. Clearwater, B.Sc

A thesis submitted in partial fulfilment

of the requirements for the degree of

Master of Science

in

Chemistry

at the

University of Canterbury,

Christchurch, New Zealand.

June 2009

ABSTRACT

Pulse Pressure Metal-Organic Chemical Vapour Deposition (PP-MOCVD) is a technique for creating thin coatings. It is less dependent on the volatility of precursors than other Chemical Vapour Deposition (CVD) processes as the precursors are introduced into the reaction chamber as an aerosol; therefore sublimation of the precursor is not necessary. This allows solutions of multiple compounds to be created with a known concentration and ratio of precursors.

We explored the formation of hydroxyapatite (HAp) coatings for use on bone implants, using a methanolic solution of calcium lactate and trimethyl phosphate (TMP) as a PP-MOCVD precursor solution. The thermal decomposition of the precursors and the reaction between them were investigated using Thermogravimetric Analysis (TGA).

Several variables on the PP-MOCVD apparatus were varied to test their effect on the formed coating: deposition temperatures, ratio of precursors, number of pulses, precursor concentration, the use of ambient temperatures and annealing the coatings after formation.

All the coatings were analysed using Scanning Electron Microscope (SEM), Energy Dispersive Spectroscopy (EDS) and Fourier Transform Infra-Red spectroscopy

(FTIR). These coatings were not uniformly smooth in appearance at the micro level. However, using higher deposition temperatures, an excess ratio of TMP to calcium lactate and annealing the coatings for short periods of time and low temperatures improved the uniformity of the coating. When vigorous annealing was performed it resulted in surface oxidation and the production of titanium dioxide (TiO_2).

The EDS results showed that both calcium and phosphorus were present in the coatings. The use of high deposition temperatures, excess TMP or gentle annealing resulted in calcium to phosphorous ratios similar to the stoichiometry of HAp. These same conditions gave improved coating uniformity.

ACKNOWLEDGEMENTS

I would like to thank my main supervisor, Associate Professor Richard Hartshorn, for his advice and support during my research. I would also like to thank Associate Professor Susan Krumdieck and Dr Susan James for their knowledge and suggestions.

I would also like to acknowledge Dr Michelle Hamilton for her help in the synthesis of the precursor compounds and Vilailuck Siriwongrungson for her guidance in the use of the PP-MOCVD and analysis apparatus.

I would like to express my gratitude towards the technical staff of the chemistry and mechanical engineering departments, in particular to Ron Tinker who has helped me fix and maintain the PP-MOCVD. I would also like to thank any other staff and students that have helped and supported me.

I extend my sincere thanks to my family who have supported me financially through my studies and by believing in my ability to achieve anything I put my mind to.

Most importantly I would like to thank my partner Blair Bonnett for always being there for me and helping me work through any problems I have.

CONTENTS

LIST OF FIGURES

LIST OF TABLES

Chapter 1

BACKGROUND INFORMATION

This project is studying the development of bio-compatible coatings for artificial bone implants to enhance their integration to the surrounding bones. This will reduce surgical recovery times, improve the life span of an implant and reduce the need for revision surgery.

1.1 Bone implants

Bone implants are devices that are placed within the body to replace a damaged section of bone and act as the missing bone would. Two areas where bone implants are needed are joint replacements and reconstructive implants.

1.1.1 Joint replacements

Joint replacement (arthoplasty) is the surgical replacement of all or part of a joint and is essential for irreversibly damaged joints.[1] One of the main causes of this

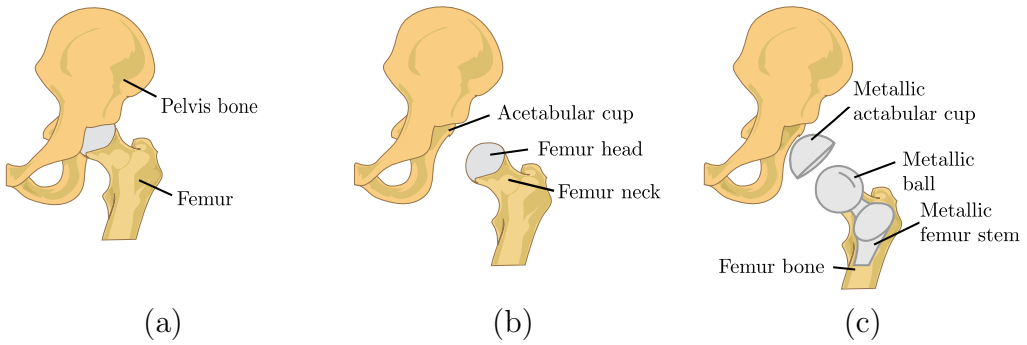

Figure 1.1: Anterior view of (a) a hip joint, (b) an expanded hip joint and (c) a hip implant.

damage is arthritis;[2] this is a condition in which the cartilage at the joints wears away causing the bones to rub against each other inflicting pain and damaging the bone. This is a common problem in elderly people due to their joints having been continuously used for a long time. Arthritis also affects physically fit people and obese people as they put a lot of strain on their joints, wearing away the cartilage.[3,4]

Hip implants are a very common type of arthoplasty with about half a million people requiring them world-wide annually.[5] The primary function of a hip joint is to support the body in stationary and active positions. Being a ball and socket joint, hip joints allow a large range of motion as they can move around an indefinite number of axes.[6] The ball of the joint is the top of the thighbone (the femur head) which moves within the hollow socket (acetabular cup) of the pelvis. These bones are connected by a layer of cartilage which serves as a protective cushion and allows the ball to glide smoothly inside the socket with low friction.[7] A hip joint is shown in Figure 1.1(a).

In a total hip replacement, a metallic acetabular cup is placed in the hip socket and the head of the femur is replaced by a metallic ball, which is anchored into

the bone by a femoral stem;[8] this is shown in Figure 1.1(c). This stops the bones from wearing each other out; as a result the patient will experience less pain and enhanced mobility. Similar methods are used in other joint replacements.

The most common procedure to fix the implant in place is to use a polymeric bone cement, for example, polymethylmethacrylate (PMMA). This undergoes *in situ* polymerization during and immediately after implantation.[9] The problem with this method is that the cement is only effective for a number of years before failures start to occur; about 10-15% of all hip replacements need to be replaced within 10-20 years.[10] This is due to wear and tear on the joint causing fracturing of the bone cement and destruction of the bone (osteolysis), forming particles in the body. As the body removes these particles, the bone grows away from the implant causing loosening. Revision surgery is then required to replace the implant. As the original implant and cement must be removed during the surgery, the bone can be damaged in the procedure. The presence of damaged bone results in patients experiencing much longer and more painful recovery periods. Additionally, the presence of particles of foreign material in the body can cause infection.

1.1.2 Reconstructive implants

Reconstructive implants are used to replace a damaged area of bone. These are used mainly in patients with bone cancer. While chemotherapy has dramatically improved the cure rate of malignant bone tumours,[11] surgical resection remains essential for the cure; this is done by complete removal of malignant tissue with a wide margin around the affected area to make sure all of the tumour is removed.

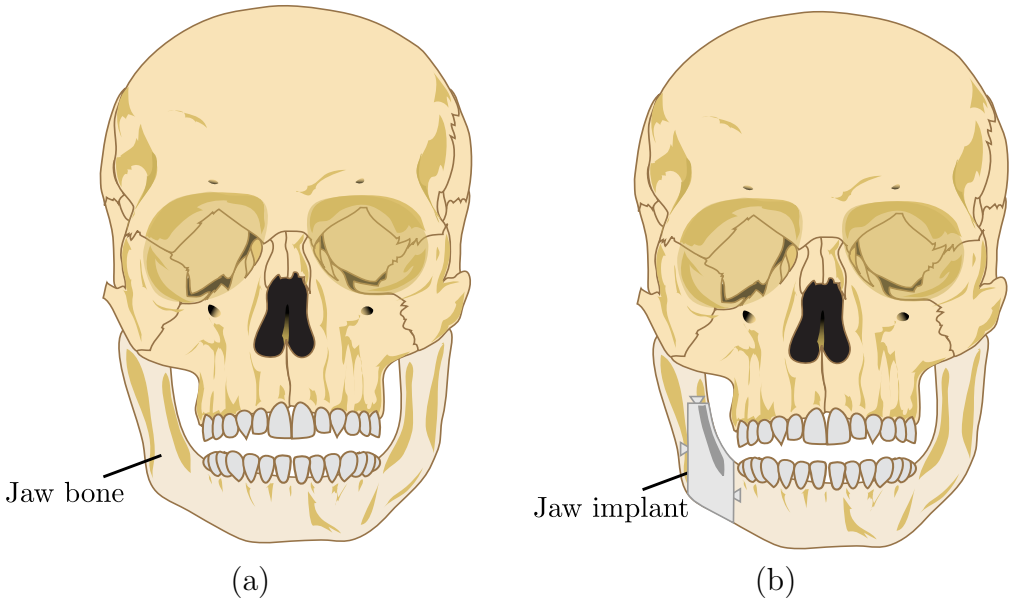

Figure 1.2: Anterior view of (a) a skull and (b) a skull with a reconstructive jaw implant.

The patient then gets a prosthetic reconstructive implant; these could be on any part of the body so some are load bearing, such as a shin implant, and some are used in repetitive motions, for example, a jaw implant[12] as shown in Figure 1.2. Due to the motion, these implants are at substantial risk of aseptic loosening (a mechanical loosening that occurs in the absence of osteolysis or infection).[13] This problem is amplified in cancer patients as the surrounding soft tissue is more likely to be damaged and therefore less supporting of the implant.

Limb-salvage surgery is now common even though amputation is the safer method as infection is a considerable problem in long bones with reconstructive implants. The desire to spare functional bone during tumor resection is especially pronounced with head and neck tumors where tissue is limited and wide margins often impact the patients's breathing, eating and speaking ability. Polymeric bone cement is used to fix the implant in place; as in the use for joint implants, it

has a limited life-span. The revision surgeries are more challenging than for joint implants as the implant must fit the bone almost perfectly, meaning the amount of damage done in the removal of the original implant must be minimised.

1.2 Bone in-growth

Bone in-growth is the ability of the bone to regenerate once the problem area has been removed. Two main areas of improving bone in-growth have been widely investigated. One is using porous metal implants[14–16] and the other is using bio-active surface coatings.[5,17]

1.2.1 Porous metal implants

Porous metal-coated implants accommodate in-growth of bone material into the pores after implantation, and thus improve fixation due to the improved mechanical interlock.[5] A porous surface can be created by spraying with a porous metal, or by coating the implant with beads or a fibre mesh.[14] The pores should be at least 100–150 μm in healthy bone or 400–500 μm in cancerous bone. If the pores are smaller, then soft tissue will form in the pores or in-growth will not occur at all.[8] However, when the pores are 300–600 μm the adhesion to the bone is faster and the strength of the interaction is strongest.[15] The problem with using porous implants is that there is an increased amount of surface area, which can produce higher levels of corrosion products. These products may have harmful biological effects when released in the body.[16]

1.2.2 Bio-active surface coatings

Many of the disadvantages of metallic implant devices can be diminished by the use of bioactive materials or coatings on the implant surface.[5] A bio-active surface coating is able to promote bonding to and integration with bone. Compounds with chemical compositions similar to bone are more bio-active. Bone is a relatively hard and lightweight inorganic material of which 65–70% is the mineral compound hydroxyapatite (HAp), $Ca_{10}(PO_4)_6(OH)_2$.[17] The other 30–35% of bone contains apatites with trace elements of magnesium, zinc, iron, carbonates and fluoride ions.[18] The trace metals are thought to play a part in cell adhesion, bone formation and bone resorption. Therefore, HAp is the more bio-active compound for this purpose and so will stimulate bone growth when placed in the body. However, it has poor mechanical properties, being weak and brittle if not supported. Due to this it is applied as a coating on an inert metal with good bio-mechanical properties, for example, titanium or titanium alloys.

Using HAp as a surface coating on implants has been successful in total joint replacements over a 15-year clinical trial.[19] Unfortunately there are still problems with these implants, the most common of which is that the current methods of applying HAp result in thick non-uniform coatings. These are prone to failures due to repeated cyclic motion, stresses and impacts on the joint which can cause the HAp to flake off in layers. This reduces the mechanical toughness of the joint, leads to implant loosening and results in HAp osteolysis in the body.

1.2.3 The next step

Both of these methods, tested separately, show improvements in bone in-growth. The next step would be to combine the methods. However, most techniques for coating implant surfaces do not give a uniform coating on a porous surface and therefore the mechanical interlock will be lost. The work described in this thesis is part of a research project that aims to combine these methods using Pulse Pressure Metal-Organic Chemical Vapour Deposition (PP-MOCVD).

1.3 Thesis organisation

Chapter 2 gives information on the two main categories (physical and chemical) of methods for coating substrates and a look into some of the different types of each. It also describes the coating method (PP-MOCVD) used in this thesis and its advantages over other methods.

Chapter 3 describes the characterisation techniques used to evaluate precursors and coated surfaces.

Chapter 4 describes the materials used in the experiments, including the precursor requirements, information on previous precursors used and the methods of forming these.

Chapter 5 provides the experimental results of a Thermogravimetric Analysis (TGA) study on calcium lactate and trimethyl phosphate.

Chapter 6 contains the PP-MOCVD experimental results.

Chapter 7 discusses the main conclusions of the research and provides some ideas for further research.

The appendices include information on the purpose of the components of the PP-MOCVD apparatus and details on how to operate the apparatus.

Chapter 2

METHODS OF COATING SUBSTRATES

Thin uniform coatings are useful and important in a large number of industrial applications, for example, forming conductors and insulators, coating optical fibers and forming wear and corrosion resistant surfaces for various materials.[20,21] There are many available methods of depositing such coatings on a range of different substrates; these are generally divided into physical processes and chemical processes, although some methods incorporate elements of both.

2.1 Physical coating processes

A physical coating process does not require any chemical reaction to occur to form a film. Instead the deposition of the film occurs due to the precursor changing through physical states. This can be done by either vapourising a solid and condensing it into a solid film (Physical Vapour Deposition (PVD)) or by melting a solid and spraying it on the substrate where it solidifies into a solid film (thermal spraying).

2.1.1 Physical Vapour Deposition

The main type of physical coating process is PVD. This involves vapourisation of a solid precursor material and transportation of the vapour through a vacuum or low pressure gaseous (or plasma) environment to the substrate. Once at the substrate the vapour condenses to form a film which can be anywhere from a few nanometers to several micrometers thick.[22] This is the dominant method for metallic thin-film deposition[23] and is used extensively in corrosion protection.[20] The vapour can be formed by various means of ejecting atoms from the solid precursor material.

Evaporation

Evaporation is a fairly straightforward and energy efficient PVD method. In a basic evaporation method, the solid precursor material sits in an open crucible, illustrated in Figure 2.1 (a). This material is heated in a high to ultrahigh vacuum to above its boiling point. As this method uses a small sample of the solid material the resulting vapour tends to travel in a concentrated beam towards the substrate, where it condenses to form a thin film.[20] A vacuum environment is used to reduce gaseous contamination in the deposition system.[22] Due to the concentrated nature of the beam it is difficult to achieve a uniform coating. This difficulty can be alleviated by rotation of the substrate, which causes the beam of material to cover different parts of the substrate.[23]

Another variant of evaporation is Molecular Beam Epitaxy (MBE), shown in Figure 2.1 (b). This uses a Knudsen cell (an equilibrium source) to hold the

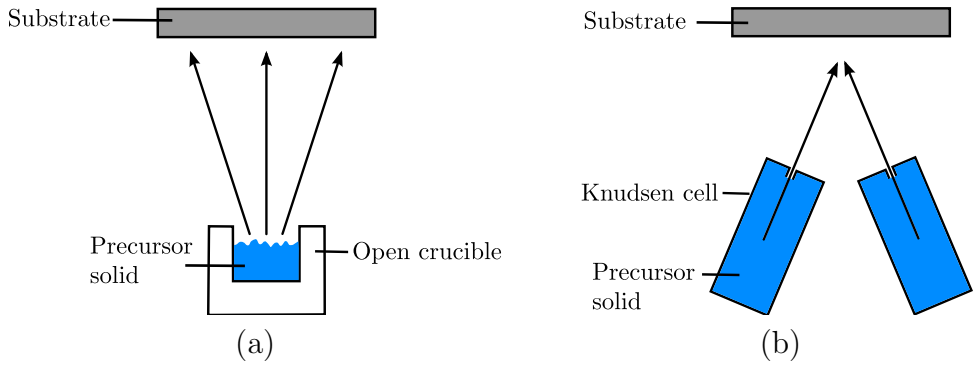

Figure 2.1: Two evaporation deposition methods using (a) an open crucible and (b) two Knudsen cells to hold the precursor solid. The latter is known as molecular beam epitaxy.

solid precursor material instead of an open crucible. Once the material is heated an atomic beam of vapour exits the cell via a tiny hole. This follows a straight line to the substrate and condenses. Using MBE instead of basic evaporation is generally preferred as the method of heating is more stable.[23]

Sputtering

Sputtering is a non-thermal PVD process where atoms from the solid precursor material are physically ejected by momentum transfer and move across a vacuum chamber to be deposited on the substrate.[20] This momentum transfer comes from argon ions (Ar^+) that are part of a glow discharge plasma; these hit the material and eject one or more material atoms in the reverse direction towards the substrate, as shown in Figure 2.2 (a). The material provides a vapourisation source, which can be mounted so it can vapourise in any direction.[22] This is performed in a low vacuum so that the sputtered atoms will experience many collisions before reaching the substrate. This process, known as thermalisation, cools down the high energy atoms so they don't cause damage to the film, the

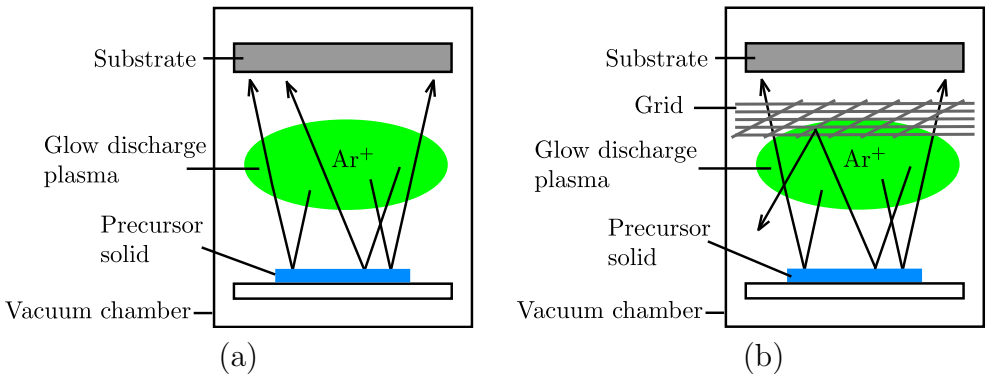

Figure 2.2: Deposition using sputtering methods. A simple set-up is shown in (a), while (b) adds a grid to perform collimated sputtering.

substrate or the structures that are beneath the substrate.[23] The downside of this is that it also reduces the flux of particles to the substrate lowering the deposition rate. Sputtering gives excellent adhesion and good composition control without using high temperatures. However, it only deposits in the line of sight and so deep holes or trenches are difficult to coat due to shadowing by other areas of the substrate. This can be overcome by using a high pressure, but at the sacrifice of the deposition rate.[20]

A variant on sputtering is collimated sputtering, illustrated in Figure 2.2(b), where a grid is placed between the solid precursor material and the substrate. This has holes slightly bigger than the precursor atoms and so does not allow any atoms that hit it at an angle to get through; instead these deposit on the reactor walls. The benefit of this method is that a more uniform coating is achieved.[23]

2.1.2 Thermal spraying

Thermal spraying involves a solid precursor material being melted to a molten or semimolten state by plasma energy or by flame. The resulting molten particles are accelerated and propelled towards the substrate.[24] Once they impact the substrate they form lamella (also known as spats) by deformation and solidification; these then bond to the surface by mechanical adhesion. The mechanical bond can be improved by performing machine roughening on the substrate before spraying.[25] Thermal spraying covers a large area at a high deposition rate, compared to PVD. However, it forms thick coatings as subsequent impacting particles build on previously deposited layers.

Plasma spraying

Plasma spraying is a relatively inexpensive and widely used method of thermal spraying. The main use of plasma spraying is in forming thick coatings to ensure adequate protection of metals from corrosion.[20] The precursor is atomised and injected into a plasma jet,[26] which is then accelerated towards the substrate with the aid of an inert carrier gas.[24] This process is shown in Figure 2.3. Plasma spraying is a very versatile method able to apply many different coatings to many different substrates. However, there are a lot of precise parameters to control to get the right coating; even a slight deviation from optimal conditions can lead to poor melting of the precursor or the modification of its composition due to partial evaporation.[27]

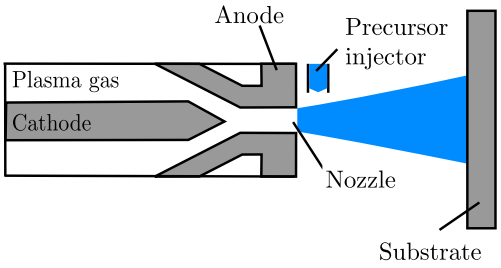

Figure 2.3: A simple diagram of a plasma jet apparatus.

Flame spraying

Flame spraying is a method of thermal spraying where a combustion flame is used to melt the precursor. A simple flame spraying set-up is shown in Figure 2.4 (a), while Figure 2.4 (b) shows a High Velocity Oxy-Fuel (HVOF) version of flame spraying. This is the preferred method as it gives a higher spray velocity than other flame spraying techniques, resulting in deposits containing stronger bonds. The solid precursor material is placed in a chamber of very high pressure, which then propels the material through a small hole in the chamber to form a supersonic gas jet.[24] This method has an advantage over plasma spraying, as it is able to form dense, well-bonded coatings using metal and alloy precursors. However, the porosity and non-uniformity of the coating can be quite high.[27]

2.2 Chemical coating processes

The important characteristics of a chemical coating process are that the coating is formed by a chemical reaction occurring on or in the area of the substrate

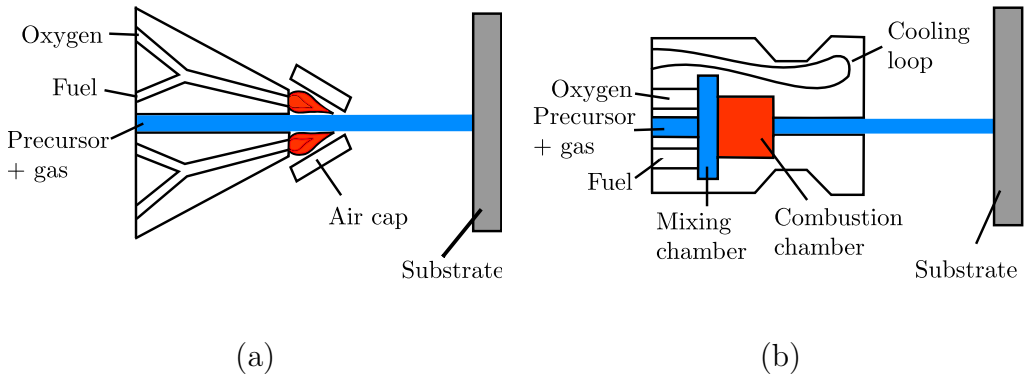

Figure 2.4: Flame spraying methods using (a) a simple flame jet apparatus and (b) a HVOF version of a flame jet.

surface and that the bond of the precursor to the substrate is based on adhesive forces.[28] Chemical coating processes are performed by covering the substrate with a liquid followed by either a thermal decomposition period or a chemical reaction to solidify the film, or by dissociation of a precursor vapour onto the substrate.

2.2.1 Wetting processes

Wetting processes are the most flexible and easily performed coating methods. They deliver highly reproducible, crack-free coatings that can be used for a variety of applications. The only prerequisite is that the solution containing the precursor must wet the substrate rather than forming droplets; using a rough substrate helps this.[29] The liquid coating is physically and chemically absorbed on to the surface and then dried and decomposed by heat and chemical reactions.[30] Only thin coatings are easily developed, but the process can be repeated multiple times to produce thicker coatings.[31]

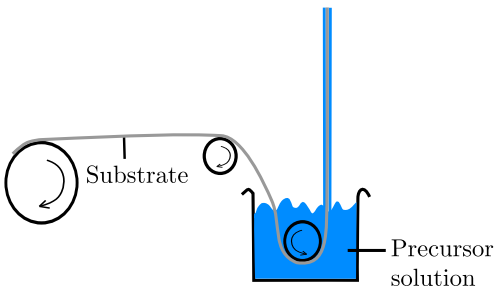

Figure 2.5: A simple dip coating set-up.

Dip coating

Dip coating is a simple, low-cost wetting process. The substrate is immersed into the solution containing the precursor and then withdrawn at a controlled rate, as shown in Figure 2.5. The thickness of the film is controlled by competing forces; gravitational force, inertial force and disjoining pressure are all working to pull the coating liquid off the substrate as it is moved out of the bulk solution. The forces acting on the coating liquid to keep it on the substrate are its viscosity and surface tension.[32] After removal from the bulk solution, the substrate is dried and decomposed resulting in a self-assembled thin film. While the remaining solvent is removed the solution reacts with the substrate and environment around it, meaning any changes in the conditions around the substrate will change the uniformity of the coating.[29] The advantage of this method is its ability to coat large areas, complex shapes and both sides of the substrate.[31]

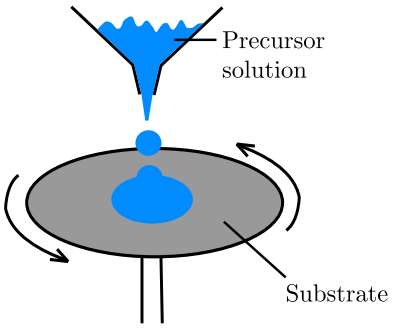

Figure 2.6: A simple spin coating set-up.

Spin coating

Spin coating is a wetting procedure where the coating material is a solution which is deposited in the centre of the substrate. This substrate is spun until the solution covers the substrate due to the centrifugal force as seen in Figure 2.6. Once this is done the spin speed is accelerated causing the excess liquid to flow to the edges. This is done until interfacial and viscous effects balance the centrifugal forces whereupon a thin liquid film remains.[29] As in dip coating, the remaining solvent then is removed either by heating or by a chemical reaction, resulting in a solid film. Coatings tend to become uniform in thickness as they get thinner; once a film is uniform it tends to remain so with further thinning.[32] If a slower speed and/or a shorter spin time is used a thicker coating is formed; this is usually not as uniform as a thinner coating since the centrifugal force is not as strong and so will not pull the solution off the edges.[31]

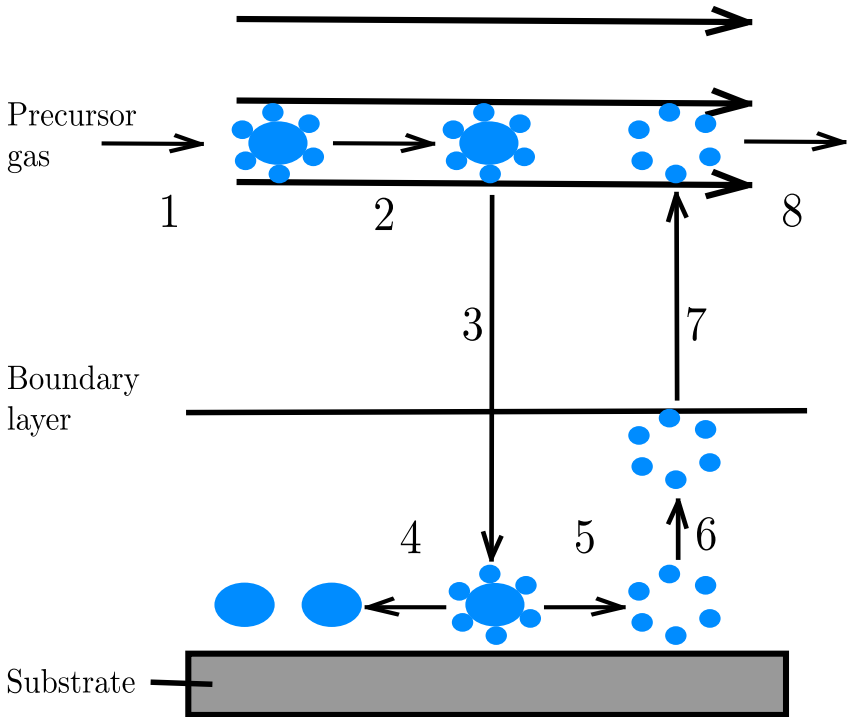

Figure 2.7: Steps in a CVD process.

2.2.2 Chemical Vapour Deposition

Chemical Vapour Deposition (CVD) is one of the most important methods for creating thin coatings because a wide range of chemical reactants and reactions can be used to deposit a large number of different types of coatings for a wide range of applications. The process of CVD is one in which a volatile compound of the element or substance to be deposited is vapourised. This vapour can react with other vapours or thermally decompose at the heated substrate to form a solid deposition on the substrate.[20,33,34]

Most CVD reactions follow a sequential step process as shown in Figure 2.7:

1. The reactants are vapourised by heating.
2. The reactant vapours enter the reactor by a forced gas flow.
3. The gases then diffuse the boundary layer by a means of mass transport to the substrate.
4. Once at the surface of the substrate the reactive species of the gas are adsorbed (physically and chemically).
5. The gas then dissociates forming the deposited material and by-products on the surface.
6. The by-products are desorbed leaving a film of wanted composition on the surface.
7. The by-products then diffuse through the boundary layer away from the substrate.
8. This by-product is then evacuated by the forced gas flow.

The boundary layer, which the reactants and by-products must pass through, is the region in which the flow velocity changes from zero (at the deposition surface) to that of the bulk of the gas. It is desirable to have a thin boundary layer to allow for easier diffusion.[35]

There have been many different variations of CVD developed in recent years. Each is aimed at improving some aspect of the deposited coating, for instance, a reduction in the level of contamination or an increase in the types of precursors and substrates that can be used.

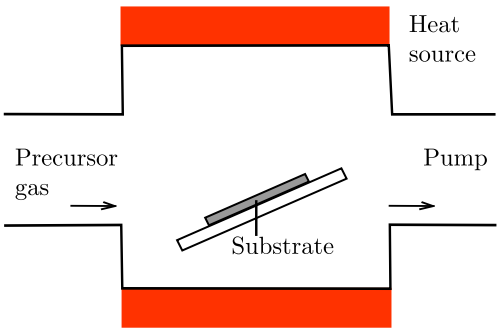

Figure 2.8: A simple hot-walled CVD apparatus.

Hot-wall reactors

A hot-wall reactor is essentially an isothermal furnace which is heated, often by resistance elements.[20] This is shown in Figure 2.8. The benefit of this method is that it supplies a uniform, easily controlled temperature on the substrate and in the gas phase. This results in a highly uniform film which can be controlled to give thick or thin films. Hot wall reactors have become increasingly popular due to the ease of obtaining high quality layers.[36] The disadvantage is that the deposition occurs everywhere (including on the reactor walls); this requires the use of disposable liners or thorough cleaning of the reactor to remove any chance of contamination.

Cold-wall reactors

In a cold-wall reactor the substrate is heated while the rest of the reactor remains cool, as seen in Figure 2.9. Heating is accomplished by induction or by high intensity radiation lamps.[33] As most CVD thermal decomposition reactions are endothermic, deposition will prefer to take place on the surface with the high-

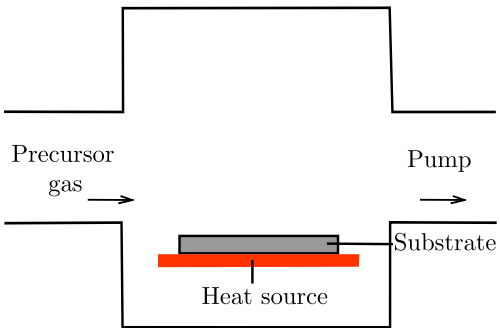

Figure 2.9: A simple cold-walled CVD apparatus.

est temperature. Therefore, the deposition in a cold-wall reactor will be focused on the substrate and not on the reactor walls. This reduces the risk of particles breaking loose from the walls and creating lumps on the substrate. The disadvantage of this method is that, due to the temperature gradient near the substrate surface, natural convection can occur, resulting in non-uniform layers.[34]

Atmospheric Pressure CVD

Atmospheric Pressure Chemical Vapour Deposition (APCVD) does not need a reactant gas pressure, which leads to it not needing a turbo pump or to be vacuum sealed.[37] This causes APCVD to be simpler and therefore cheaper than other forms of CVD; it is also able to run faster. With recent developments, the quality of the deposits has been considerably improved and satisfactory deposits of many materials have been obtained.[20]

Low Pressure CVD

There are two types of CVD which operate at a lower pressure than APCVD. These are Low Pressure Chemical Vapour Deposition (LPCVD), which uses a pressure of 0.5–1 Torr, and Ultra-High Vacuum Chemical Vapour Deposition (UHVCVD), which typically uses pressures of the order of 10^{-5} Torr. For these methods a vacuum pump is required and the reactor must be vacuum sealed; this causes these methods to be more costly than APCVD.[20] The benefit of the extra cost is that the vacuum lowers the deposition temperature needed and reduces the amount of impurities in the chamber. This technique provides deposits with greater uniformity, better step coverage and improved quality compared to atmospheric pressure CVD. The main disadvantage is that the lower the pressure in the system, the lower the deposition rate.[38]

Laser enhanced CVD

Laser Enhanced Chemical Vapour Deposition (LECVD) is a method where laser beams enhance and control reactions at the substrate to form a film. There are two types of LECVD processes: pyrolytic and photolytic. The former uses simple optics to focus and direct a laser beam to heat the substrate; this in turn heats the precursor gas causing it to decompose, as shown in Figure 2.10 (a). This deposition is similar to that resulting from using a cold wall reactor.[33] In this LECVD method the substrate needs to be carefully chosen so that it melts above the precursor gas decomposition temperature used.

The photolytic process uses energetic photons to disassociate the gas molecules,

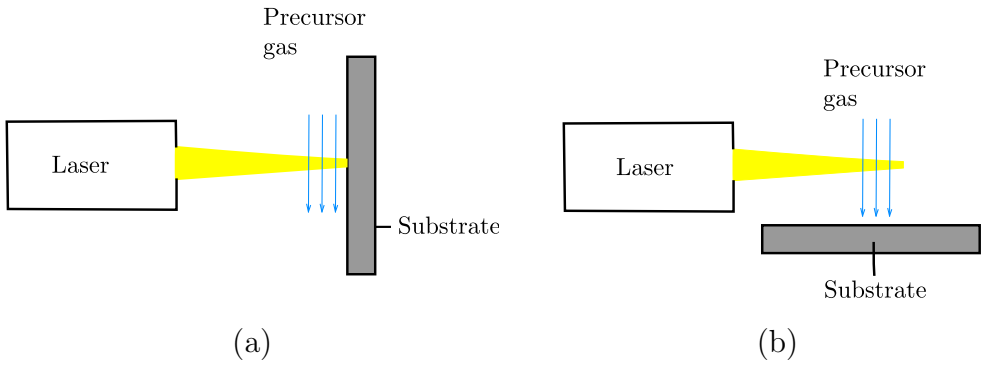

Figure 2.10: LECVD methods (a) uses a pyrolytic set-up and (b) uses a photolysis set-up.

which then deposit on the substrate.[39] This method is shown in Figure 2.10 (b). In many cases ultra-violet (UV) radiation is required to initiate the dissociation reactions; UV lamps can be used for this but more energy is obtained from UV lasers. The gas molecules absorb this energy, either directly or indirectly, via a photosensitiser.[40] As this method is photon-activated and works without exposing the substrate to the atmosphere, no heating is required and there is minimal risk of contamination. Therefore, there are no constraints on the type of substrate used.[20]

Plasma Enhanced CVD

Plasma Enhanced Chemical Vapour Deposition (PECVD) combines chemical and physical vapour deposition processes. This method uses a considerably lower deposition temperature than most CVD and PVD processes and the chemical reaction in the gas or vapour is activated by the electric discharge of the plasma.[41] The disadvantage of PECVD is that it is difficult to obtain a deposition of pure materials as in most cases desorption of the by-products and other gases is in-

complete due to the low temperature used.[20]

Metal-Organic CVD

Metal-Organic Chemical Vapour Deposition (MOCVD) is the only CVD process distinguished by the type of precursor used. A metal-organic compound is one in which an atom of a metallic element is bound to a ligand containing one or more carbon atoms of an organic hydrocarbon group.[20] The precursor is introduced into the reaction chamber and is then thermally decomposed at the heated substrate in a cold wall reactor. The precursor must be volatile at relatively low temperatures (between 300–800°C) and pressures between 1 Torr and atmospheric pressure. MOCVD precursors are in the gas phase and so it is possible to control the flow rate and partial pressures allowing for reproducible depositions; hence this can be readily adapted for mass production in industry. The main disadvantage is that, due to using an organic precursor, carbon contamination can become a problem.[42]

Pulse Pressure-MOCVD

PP-MOCVD is a direct liquid injection system where a solution of a metal-organic precursor is pulsed through an ultrasonic nozzle into a cold wall reactor. A simple diagram of this is shown in Figure 2.11. The ultrasonic nozzle produces small droplets (about 15 μm in diameter) from the solution, which flash evaporate immediately after injection. The precursor diffuses through the chamber to the heated substrate where it decomposes and forms a thin film.[43,44] Each pulse

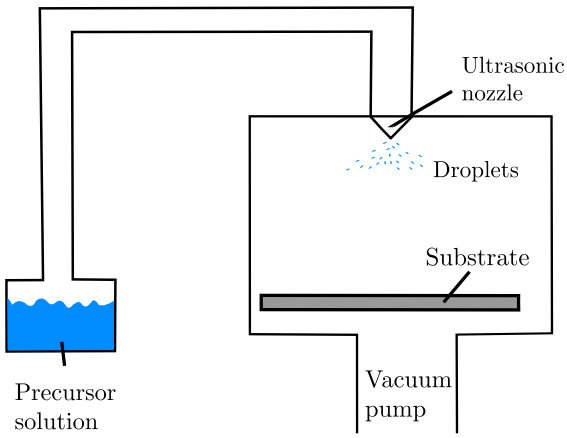

Figure 2.11: A simple diagram of a PP-MOCVD apparatus; see appendix A for a more detailed diagram.

supplies an exact volume of solution, of known concentration. During each pulse cycle the precursor solution is injected into the reactor chamber causing a sharp increase in pressure as the droplets evaporate; this is quickly reduced with the aid of a vacuum pump.[45] This is shown in Figure 2.12.

PP-MOCVD has the same advantages as standard CVD,[20,35] including:

- It is not restricted to a line of sight deposition, but it can form high density pure coatings with good step coverage of deep recesses, holes and other difficult three dimensional configurations.
- Thick coatings (mm) can be readily obtained and are cheaper than PVD processes.
- There are many variables which can be changed, allowing changes to the composition to occur during deposition.

However standard CVD has the following disadvantages:

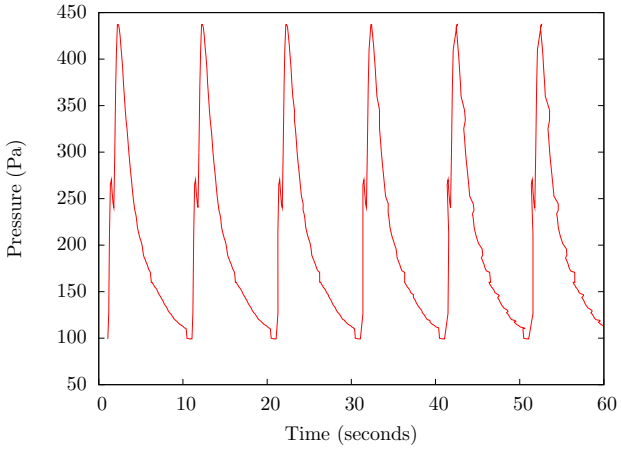

Figure 2.12: A representation of the pulse pressure flow cycles.

- The substrates must be heated to high temperatures (above 600°C). There are not many substrates that are thermally stable at these temperatures.
- The reactants and by-product vapours are often hazardous, toxic and corrosive.
- There can be growth rate and uniformity problems, especially on large 3D substrates.

The PP-MOCVD overcomes these disadvantages by having more control of the morphologies of the thin film, as it is capable of changing many variables. Using metal-organic precursors greatly reduce the risk of hazardous, toxic and corrosive vapours being produced and do not require such high temperatures to decompose, thereby allowing more types of substrate to be used.[35,46]

PP-MOCVD also has the benefit that the precursor is introduced as a solution and not as a vapour. In a fixed flow CVD the precursor is sublimed and passed through the tubing using a carrier gas; this affects the concentration of the precursor that

enters the reaction chamber. Also all the tubing and the mixing chamber in fixed flow CVD must be kept at a temperature above the evaporation temperature of the precursor in order to stop condensation.[45]

Using PP-MOCVD the concentration ratios of the vapour is the same as the liquid it came from as there is no need for a carrier gas. The solution can contain more than one precursor, allowing exact pre-determined ratios of precursors to be used. By contrast, in standard CVD each precursor must be sublimed separately and combined in the mixing chamber, making it difficult to control the ratio of the precursors.

Uniformity and growth rate are affected by the pressure the system uses. A high pressure gives a faster growth rate but a poor coverage due to viscous and thermal effects. By contrast, a low pressure gives a better coverage on flat and complicated substrates, although at a slow growth rate.[47] As PP-MOCVD uses high and low pressures it can form thin uniform coatings on either smooth or porous substrates and is cheaper to run. This has not been achieved with any previous CVD technology.

For these reasons, PP-MOCVD will be the method used for this research in attempts to form thin, uniform HAp coatings on titanium substrates.

Chapter 3

CHARACTERISATION TECHNIQUES

The calcium precursor compounds were characterised using Fourier Transform Infra-Red spectroscopy (FTIR), TGA and elemental analysis. The PP-MOCVD coatings were characterised by FTIR, Scanning Electron Microscope (SEM) and Energy Dispersive Spectroscopy (EDS). This chapter gives a brief outline of how these techniques work.

3.1 FTIR

FTIR is a method where infra-red radiation causes the atoms within the sample to vibrate relative to each other. A molecule can only exist in distinct vibrational states with defined energies. The differences in the energies of these states allow analysis of the vibrational character of the bonds in the sample.[48] In this research, diffuse reflectance FTIR was used; this is where multiple infra-red beams are bounced directly off the sample surface and compared to a background.[49] When analysing coatings, the thickness of the coating is important as if the film is too thick the infra-red beams will not be able to penetrate through to the substrate

underneath. If the film is too thin then the spectrum obtained is weak and hard to analyse.

3.2 TGA

TGA is a simple analytical technique that is performed on samples to determine thermal stability and monitor decomposition or other chemical reactions. This is done by monitoring the weight change that occurs in the sample as a function of increasing temperature. The weight can be lost through simple processes, such as drying, structural water release, structural decomposition, carbonate decomposition, gas evolution, sulfur oxidation and fluoride oxidation.[50] Since PP-MOCVD involves thermal decomposition of precursor molecules, TGA studies could provide an insight into the chemistry that may be occurring in the reaction chamber of the PP-MOCVD.

For this research a horizontal balance TGA instrument was used; a simple diagram of this is shown in Figure 3.1. This is an instrument which consists of an analytical balance and a furnace chamber. The analytical balance has two arms; one holds the sample cup and the other holds the reference cup. These are both inserted into the furnace chamber. The cups are tared before the sample is inserted to give an accurate measure of the weight of the sample. The analysis is performed in a nitrogen atmosphere. The data from this instrument are normally displayed as a plot of percentage weight loss as a function of increasing temperature.

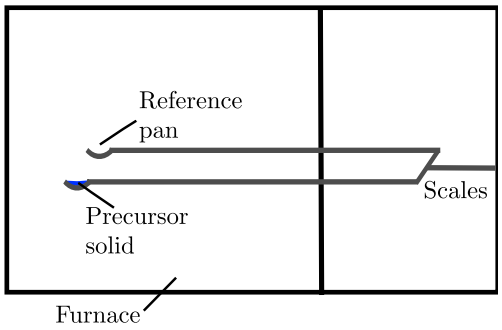

Figure 3.1: Diagram of a horizontal TGA apparatus.

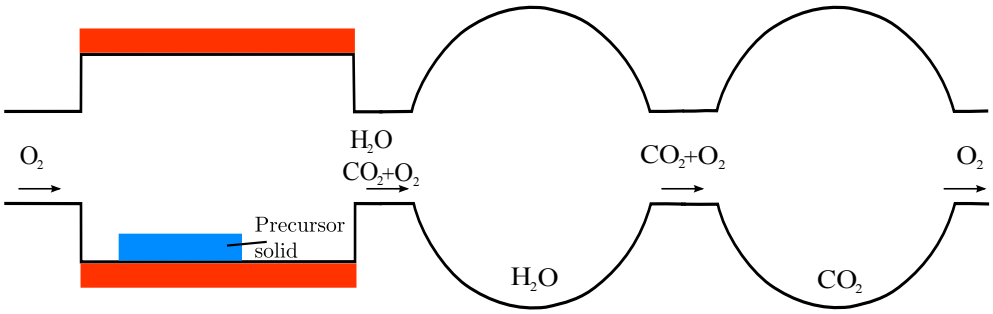

Figure 3.2: Elemental analysis set up.

3.3 Elemental analysis

Elemental analysis is a technique for determining the empirical formula of an unknown compound. For this research, combustion analysis was performed. In this method, a stream of hot oxygen gas is passed over a sample of known mass. The elements in the sample react with the oxygen to form gases; hydrogen reacts to form $H_2O_{(g)}$ and carbon reacts to forms $CO_{2(g)}$. Each of these gases are caught in separate traps, as shown in Figure 3.2. The mass of each gas is calculated by the mass gain in the trap.[51] By comparing the mass gain in each trap to the original sample mass, the empirical formula can be calculated.

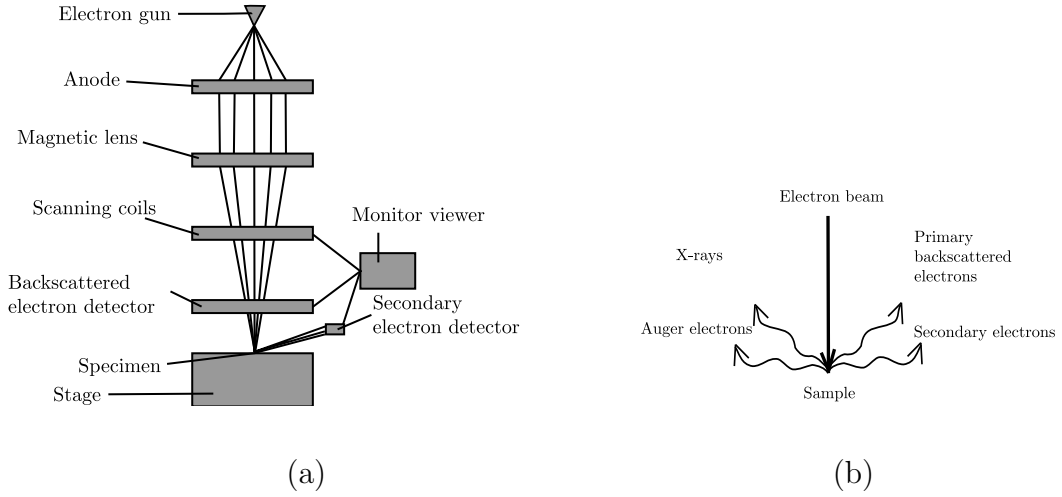

Figure 3.3: (a) Schematic of an SEM apparatus and (b) SEM electron beam reaction with the sample.

The elemental analysis in this research was performed by the Campbell Microanalytical Laboratory at the University of Otago.

3.4 SEM

A SEM is an instrument which delivers images of a surface by scanning it with a high energy beam of electrons. A simple schematic of a SEM is shown in Figure 3.3(a). The beam is focused by a range of magnetic lenses within the vacuum chamber. A set of scanning coils moves the beam across the sample in parallel lines. When the beam hits a point on the sample, electrons and X-rays are emitted, as seen in Figure 3.3(b). A detector counts the X-rays, back-scattered electrons and the secondary electrons and converts them into a signal which is amplified and shown on a computer screen.

3.5 EDS

EDS is an analytical technique which determines the elemental composition of the sample. It is coupled to the SEM apparatus and accurately measures the amount of energy of an X-ray when it is absorbed in a silicon sensing element.[52]

The electron beam excites an electron in an inner orbital, causing it to be emitted from the atom, creating an electron hole. An electron from an outer (higher energy) shell fills this hole, as shown in Figure 3.4. The energy which is lost by this process is emitted as an X-ray. The detection of these X-rays is key to EDS, as it uses the measured energy of the emitted X-ray to identify the elements present in the sample. It will also count the number of X-rays photons and give an approximate measure of the amount of each element, thus allowing the composition of the sample to be determined.

In this research the elements present are carbon, oxygen, phosphorus, calcium and either titanium or silicon for a surface analysis. The powder resulting from the TGA studies can also be analysed by EDS. In this method the powder sample is adhered to carbon tape so there is no titanium or silicon present, but if the sample is very thin or the tape is visible then there will be more carbon shown in the analysis than present in the sample.

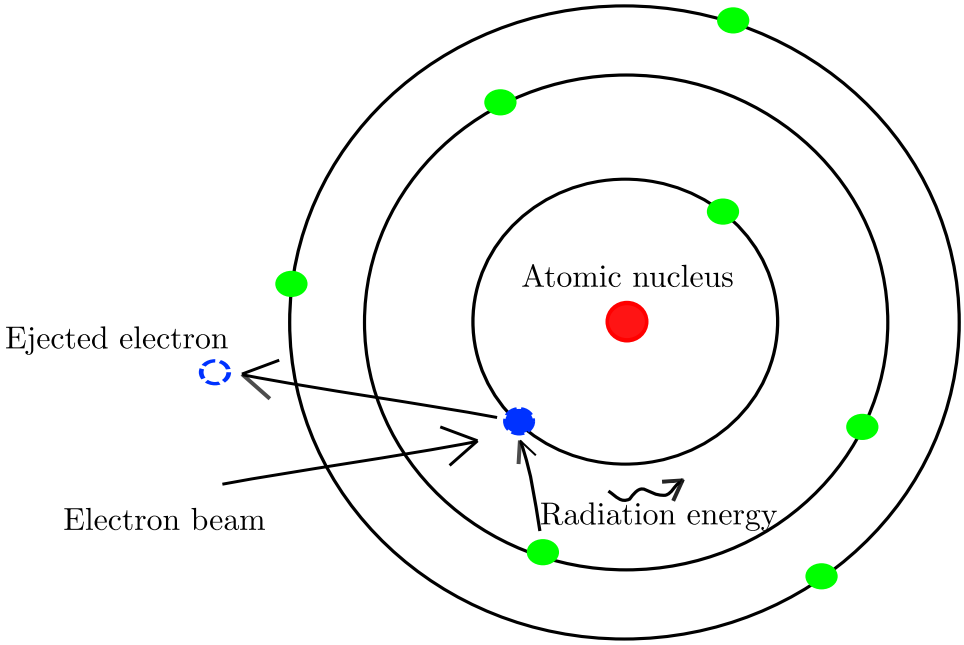

Figure 3.4: Diagram of EDS affect on an atom and how X-rays are emitted.

Chapter 4

PP-MOCVD PRECURSOR COMPOUNDS

The aim of this research is to form a HAp coating on a substrate compatible with implants. Medical implants are usually composed of titanium as it is a lightweight metal which has a high corrosion resistance and mechanical properties which resemble bone.[53] Therefore, titanium substrates were mostly used. However, some samples used silicon substrates due to a lack of titanium substrates.

An ideal PP-MOCVD precursor is a metal-organic compound, i.e., a compound which contains a metal atom bound to one or more organic ligands. Since it is supplied to the reaction chamber as part of a liquid phase, the precursor must be soluble, otherwise it will clog the ultrasonic atomisation nozzle. The solvent must be volatile so as to evaporate before the decomposition of the precursors.[47] The precursor must be thermally active and able to decompose at low substrate temperatures in cold wall reactors.[45] Using a precursor with a high vapour pressure will result in higher growth rates as a higher concentration of the precursor in the solvent can be used.[54]

In this research, the precursor must form hydroxyapatite on the substrate. Therefore, there must be a source of calcium and phosphate. The phosphate source

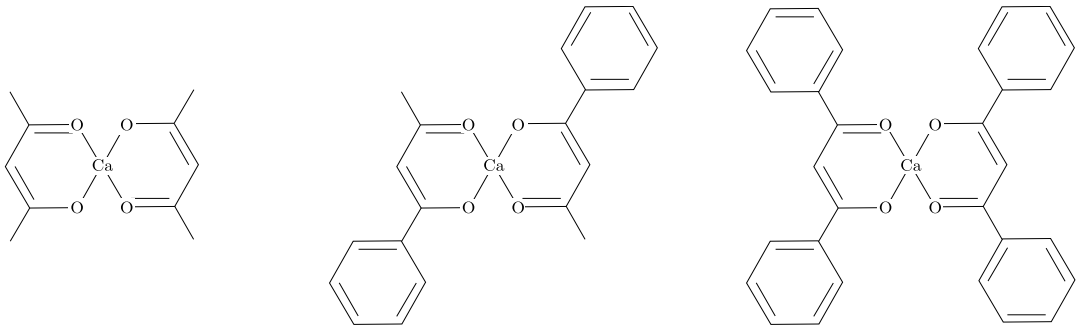

(a) calcium acetylacetone (b) calcium benzoylacetone (c)calcium dibenzoylmethane

Figure 4.1: Previous PP-MOCVD calcium precursors.

used is trimethyl phosphate (TMP) and the calcium source is a metal-organic compound, a small variety of which have been looked at in earlier work.

4.1 Previous precursors

Previous calcium precursors used in forming hydroxyapatite films with MOCVD consist of β-diketone ligands coordinated to a calcium ion;[55,56] such precursors were also used in a previous PP-MOCVD study.[57] In this study the three compounds which were tested were bis(2,4-dioxopentan-3-ido)calcium (calcium acetylacetone), bis(1-phenyl-1,3-dioxobutan-2-ido)calcium (calcium benzoylacetone) and bis(1,3-diphenyl-1,3-dioxopropan-2-ido)calcium (calcium dibenzoylmethane), all of which are shown in Figure 4.1.

Methanol was used as the solvent as it is a volatile organic solvent which has proven to be successful in previous experiments with PP-MOCVD. Hartshorn *et al* showed that the calcium dibenzoylmethane was the most soluble of the three precursors in methanol making it the most appropriate calcium precursor

out of the three tested.[57] In this study a precursor solution of five parts calcium dibenzoylmethane plus three parts TMP was dissolved in methanol at a concentration of 0.08mole% calcium dibenzoylmethane, calculated using the following equation:

$$C_{\text{Solution (mol\%)}} = \frac{n_{\text{Calcium precursor (mol)}}}{n_{\text{Calcium precursor (mol)}} + n_{\text{solvent (mol)}}} \tag{4.1}$$

This precursor solution was deposited on the surface of a titanium substrate using PP-MOCVD. This was repeated three times and the EDS showed that the substrate after PP-MOCVD was rich in calcium and phosphate in some areas, indicating that both precursors were able to deposit and adhere to the substrate. However, it did not give a uniform, smooth coating; possible causes include the concentration of the precursor solution being too low or the ratio of compounds, decomposition temperature, pulse volume or the number of pulses not being ideal.[58]

4.2 Synthesis

The initial synthesis and purification procedure was carried out following the Hartshorn *et al* calcium dibenzoylmethane preparation; this involved dissolving dibenzoyl methane (dbm) in distilled water and adding drop-wise with stirring to calcium hydroxide ($Ca(OH)_2$).[57] The calcium dibenzoylmethane compounds formed by this method were not reproducibile and $Ca(OH)_2$ was present. The use of more forcing conditions lead to improved reproducibility. The dbm was dissolved in ethanol (or methanol) and added drop-wise to calcium hydroxide ($Ca(OH)_2$). The resulting solution was then refluxed, followed by being cooled in

ice. This was then filtered leaving a white precipitate which was analysed to be the calcium complex with some unreacted $Ca(OH)_2$.

To remove the unreacted $Ca(OH)_2$, the product was purified by mixing with water as neither dbm or $Ca(OH)_2$ are particularly soluble in water. This was then filtered to separate the product from the unreacted reactants and the solvent was removed to leave the purified product. The FTIR spectra of the purified product revealed that the ligands initially present in the calcium complex exchanged in water. A different purification method was tried involving the filtration of a saturated solution in hot ethanol and analysed showing that the dbm ligands had been converted to benzoate so the product was no longer calcium dibenzoylmethane. As the formation of purified calcium dibenzoylmethane was unsuccessful this line of work was no longer pursued.

4.2.1 Alternative precursors

The overall aim of this work is to form a coating for a bone implant therefore, the coating must be able to be put in the body without the risk of causing medical problems. The primary alternative precursor investigated was calcium lactate. This was due to it being a naturally occuring compound that is unlikely to cause any harm to the body.

Initially the precursor solutions were prepared using a similar synthesis to that used for calcium dibenzoylmethane.[57] The material formed from initial synthesis was inconsistent, the melting points ranged from melting at 190°C to burning at 330°C. This is clearly not calcium lactate. However, using forced synthesis

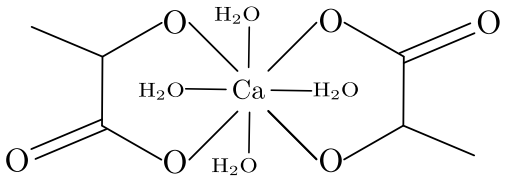

Figure 4.2: An example of the possible structure of the calcium lactate precursor. As calcium is known to prefer relatively high coordination numbers, the lactate ligands are thought to be attached in a chelating fashion.

conditions, the calcium lactate was repeated and the FTIR and melting points were consistent; however, the product contained varying amounts of $Ca(OH)_2$. This showed promise in the formation of calcium lactate.

4.2.2 Final synthesis and results

The final synthesis involved adding 3.75 mL of lactic acid to 500 mL of distilled water. The resulting solution was added drop-wise with stirring to 1.85 g of $Ca(OH)_2$. This was left to reflux in an oil-bath for five days. The solvent was removed and the remaining compound was dried in vacuo over fused calcium chloride ($CaCl_2$). The calcium lactate compound formed by this method was reproducible and characterised using melting points and by FTIR.

Solubility tests were performed which found that the maximum concentration of the precursor to be used in the PP-MOCVD was 0.004 mole%. Commercially made calcium lactate from BDH Chemical Ltd was found to have a higher solubility; the maximum precursor concentration formed from it was 0.47 mole%. This is 100 times greater than the synthesised calcium lactate. This could be due to different crystalline forms, or different particle sizes. This was not investigated

and the commercial material was subsequently used.

Chapter 5

THERMOGRAVIMETRIC ANALYSIS RESULTS

The formation of hydroxyapatite via PP-MOCVD requires a calcium precursor and a phosphate precursor. In this research calcium lactate and TMP were to be the precursors used for PP-MOCVD. TGA experiments were performed on calcium lactate and TMP in order to understand the chemistry of their decomposition and to establish whether their behaviour changed in the presence of each other and when different calcium lactate to TMP ratios were employed. These experiments gave insight into the temperature at which the calcium lactate and the TMP would react with each other, the decomposition path of the compounds, and the temperature at which hydroxyapatite may be formed.

The TGA apparatus was set with a linear temperature ramp of 1°C/min to ensure that all the details of the weight change were observed. A run was performed ramping the temperature from room temperature to the maximum temperature (1500°C) of the TGA. This showed that the decomposition of calcium lactate was completed by 800°C. Hence all runs performed in this study went up to 800°C unless otherwise stated.

To assist with the analysis of results, a derivative of the decomposition curve was plotted; each trough in the derivative represents a point of maximum weight loss. The highest points between the troughs were transposed to the TGA curve and used to define the start and finish of each weight loss step. These weight loss points were averaged over all the repeats of this experiment. The results presented in this chapter are averages over all equivalent runs performed, with an error given at twice the standard deviation.

There are many sources of error in using the TGA; for example, the sample or reference cup may not be completely clean from a previous run affecting the weight loss as the remaining substance may decompose during the run. Additionally the TGA is very sensitive and vibrations that occur while it is running can affect the measurements.

5.1 Calcium lactate

The commercially available calcium lactate used for these experiments claimed to contain calcium lactate plus five water molecules ($Ca(C_3H_5O_3)_2.5H_2O$). Elemental analysis was performed on a sample of this calcium lactate; the results, shown in Table 5.1, were not consistent with the sample containing five water molecules. For this compound to be calcium lactate there must be one calcium atom; from the percentage of the calcium present, the molar mass of the compound is $291.92\,\mathrm{gmol}^{-1}\pm2.2\,\mathrm{gmol}^{-1}$. Calcium lactate also consists of six carbon atoms from which the compound's molar mass is $291.77\,\mathrm{gmol}^{-1}\pm2.1\,\mathrm{gmol}^{-1}$. The average of these two numbers ($291.85\,\mathrm{gmol}^{-1}\pm4.3\,\mathrm{gmol}^{-1}$) was used to work out

Element	$CaC_6O_6H_{10}$ $5H_2O$	Elemental Analysis Average	$CaC_6O_6H_{10}$ 4.1 H_2O
Carbon %	23.38%	24.70%±0.09%	24.67%
Hydrogen %	6.54%	6.32%±0.07%	6.28%
Calcium %	13.00%	13.73%±0.05%	13.72%
Oxygen %	57.09%	55.24%±0.14%	55.32

Table 5.1: The percentage of elements expected for calcium lactate with five water molecules attached and the results of the elemental analysis.

the number of hydrogen atoms to be 18.3±0.5. Since there are ten hydrogen atoms in calcium lactate the remaining 8.3±0.5 must form part of the attached water molecules. Similarly the number of oxygen atoms was calculated to be 10.1±0.2 which means 4.1±0.2 are part of the attached water molecules. Both of these results are consistent with there being 4.1±0.7 water molecules attached to the calcium lactate; this is the number used in the following calculations.

5.1.1 Results

The TGA of calcium lactate by itself gave four weight losses at different temperature ranges, as shown in Figure 5.1. The weight loss percentages shown by the TGA were converted into the corresponding molar masses using the formula

$$M_{\text{loss}} = M_{\text{Calcium lactate}} \times \%_{\text{loss}} \tag{5.1}$$

The average of the weight losses for each step are shown in Table 5.2.

Each of these weight losses corresponds to a process, for example, drying. To determine if any of the weight losses were due to the loss of water molecules,

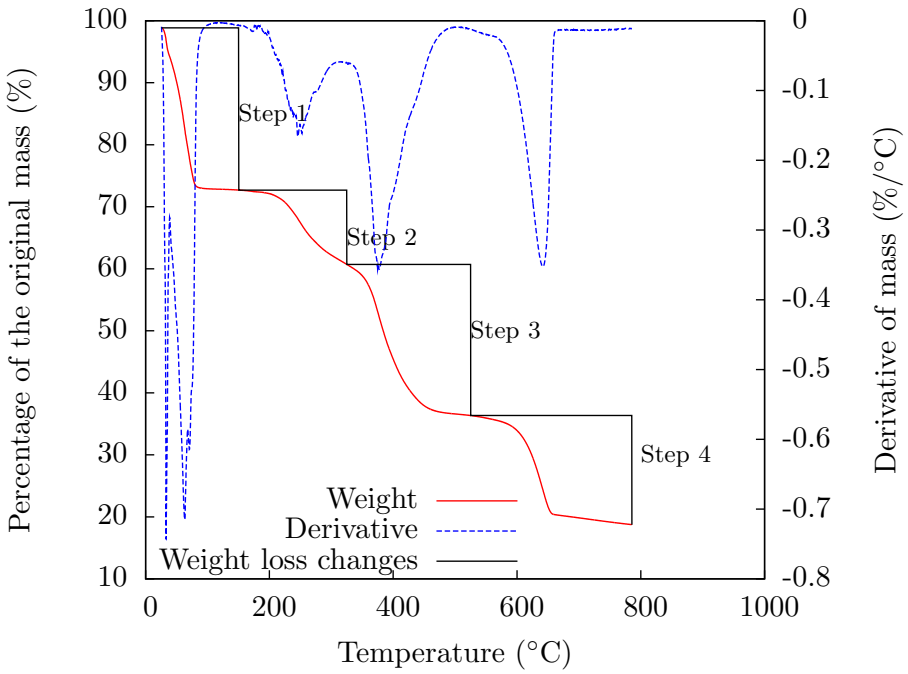

Figure 5.1: An average of the thermogravimetric analysis of calcium lactate.

Weight loss step	Temperature	Percentage	Molar mass
1^{st}	0-150°C	26.31%±0.52%	$76.88\,\mathrm{gmol}^{-1}$
2^{nd}	151-325°C	$10.54\% \pm 0.99\%$	$30.80\,\mathrm{gmol}^{-1}$
3^{rd}	326-525°C	$26.65\% \pm 1.57\%$	$77.88\,\mathrm{gmol}^{-1}$
4^{th}	526-800°C	$18.39\% \pm 1.40\%$	$53.74\,\mathrm{gmol}^{-1}$
Final	800°C	$18.03\% \pm 3.25\%$	$52.69\,\mathrm{gmol}^{-1}$

Table 5.2: Conversion of percentage weight loss to molar mass for calcium lactate.

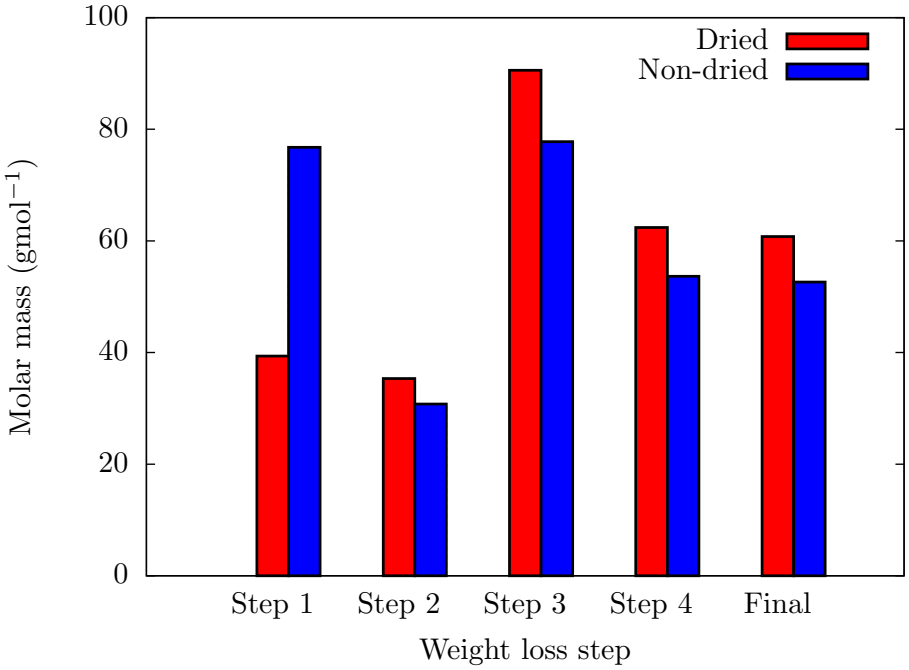

Figure 5.2: The difference in molar mass lost in the TGAs of dried and non-dried calcium lactate.

a sample of calcium lactate was dried in vacuo over fused $CaCl_2$ for four days before being put in the TGA. The weight losses of standard calcium lactate and the dried calcium lactate are compared in Figure 5.2.

5.1.2 Decomposition discussion

The first weight loss step is significantly lower in the dried calcium lactate than in the standard, whereas all the other weight loss steps are similar. The first weight loss most likely corresponds to the loss of the water molecules. For the non-dried sample this weight loss was the 4.1±0.6 water molecules and for the dried sample the weight loss was equivalent to two water molecules. The FTIR of

product after the first weight loss step was similar to the FTIR of calcium lactate except the O–H peak was not as large, thus agreeing with the prediction that the first weight loss is the loss of water molecules.

The next part that could be easily analysed was the product remaining at the end of the TGA. At temperatures greater than 800°C there was an average of 18.03% remaining; this corresponds to $52.69\,\mathrm{g\,mol^{-1}}$. The most logical compound based on the starting compound with this molar mass would be calcium oxide which has a molar mass of $56.08\,\mathrm{g\,mol^{-1}}$. A FTIR was taken of the remaining product and compared to a FTIR of calcium oxide after it had been heated to 800°C. These showed the same major peaks ($3644\,\mathrm{cm^{-1}}$, $1426\,\mathrm{cm^{-1}}$ and $864\,\mathrm{cm^{-1}}$ versus $3644\,\mathrm{cm^{-1}}$, $1417\,\mathrm{cm^{-1}}$ and $868\,\mathrm{cm^{-1}}$); therefore, the remaining product is likely to be calcium oxide.

Calcium oxide can be formed in a process known as calcination where calcium carbonate loses carbon dioxide through thermal decomposition. This would be a good candidate for the process which occurs in the fourth weight loss (18.39%±1.4% between 525–800°C). Carbon dioxide is calculated to be 14.68% of calcium lactate; this number is not within the error value. However, a FTIR of the sample remaining after being heated to 500°C was taken and compared to a FTIR of calcium carbonate after it had been heated to 500°C ($2512\,\mathrm{cm^{-1}}$, $1796\,\mathrm{cm^{-1}}$, $1458\,\mathrm{cm^{-1}}$, $874\,\mathrm{cm^{-1}}$ and $713\,\mathrm{cm^{-1}}$ versus $2512\,\mathrm{cm^{-1}}$, $1794\,\mathrm{cm^{-1}}$, $1442\,\mathrm{cm^{-1}}$, $876\,\mathrm{cm^{-1}}$ and $712\,\mathrm{cm^{-1}}$). These are very similar and therefore calcination is likely to be the occurring process.

Another common weight loss process is the release of water molecules from ligands. In calcium lactate two water molecules could be released through dehy-

dration of the two lactate ligands. If this was happening it was calculated there would be a weight loss of 12.35%, which is approximately the second weight loss step of 10.54%. The loss of these water molecules may change the lactate ligands into acrylate ligands as shown in step two of Figure 5.3. The acrylate ligands may polymerise under these conditions, but this would not affect the sample weight. The FTIR of the product from the second weight loss step showed a further decrease in the O–H peak. Due to the size of the carbonate peak at 1576 cm^{-1} it is hard to confirm if an alkene peak is present. However, this peak now has a rougher edge suggesting that it is overlapping another peak. A FTIR of calcium acrylate could not be found and therefore could not be compared.

Assuming calcium oxide is the only product left at the end, the third weight loss step must be a structural decomposition losing C_5H_6O. The calculated weight loss (28.13%) also fits in with the third weight loss (26.65%).

Calcium lactate decomposes into calcium oxide in four clear stages. The overall predicted decomposition is shown in Figure 5.3 and Table 5.3.

5.2 Trimethyl phosphate

Since TMP is the phosphorus source it is necessary to analyse how TMP acts by itself. As TMP has a boiling point of 197°C[59] the TGA was run at 1°C/min until it reached 250°C. As shown in Figure 5.4, 100% of the weight of TMP was lost in one step by the time the temperature reached 100°C, presumably due to evaporation. The weight loss which occurs is well below the boiling point of TMP

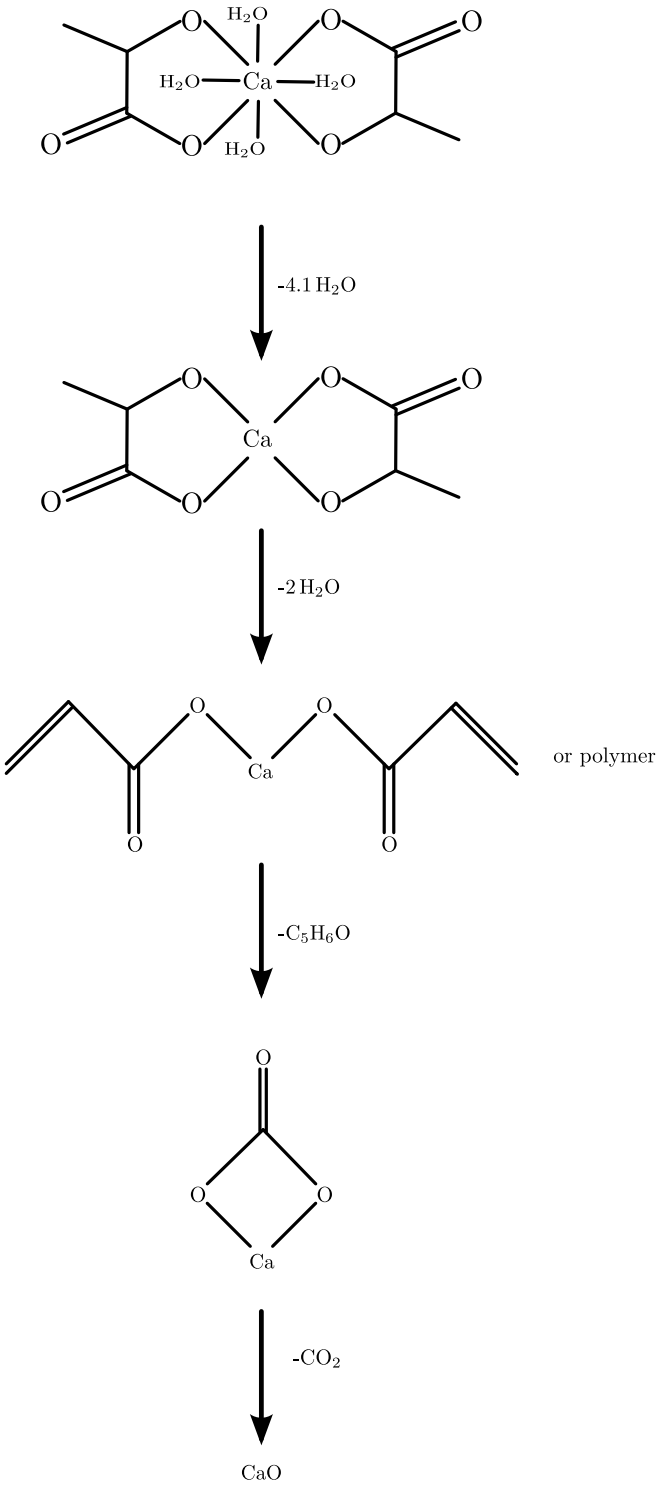

Figure 5.3: The predicted decomposition of calcium lactate to calcium oxide.

	Percentage
1^{st}	$26.31\% \pm 0.52\%$
$4.1H_2O$	$25.31\% \pm 4.31\%$
Difference	1.00%
2^{nd}	$10.54\% \pm 0.99\%$
$2H_2O$	$12.35\% \pm 0.30\%$
Difference	-1.80%
3^{rd}	$26.65\% \pm 1.57\%$
C_5H_6O	$28.13\% \pm 0.68\%$
Difference	-1.48%
4^{th}	$18.39\% \pm 1.40\%$
CO_2	$14.68\% \pm 0.17\%$
Difference	3.71%
Final weight	$18.03\% \pm 3.25\%$
CaO	$19.22\% \pm 0.13\%$
Difference	-1.19%

Table 5.3: The overall decomposition of calcium lactate: the experimental weight loss of each step, weight loss of the predicted compound and the difference between the two.

due to the flow of nitrogen over the heated liquid.

5.3 Calcium lactate and trimethyl phosphate

It would be expected that, if the TMP and calcium lactate did not react when they were mixed and heating begun, then all the TMP would be lost in the first weight loss step with the first group of water molecules. The other steps would then follow along as calcium lactate did by itself, ending in calcium oxide. Many molar ratios of calcium lactate to TMP were tested. The first of these uses the stoichiometry of hydroxyapatite (5:3, calcium to phosphate) while the others increased the amount of TMP (5:12, 5:24 and 5:60).

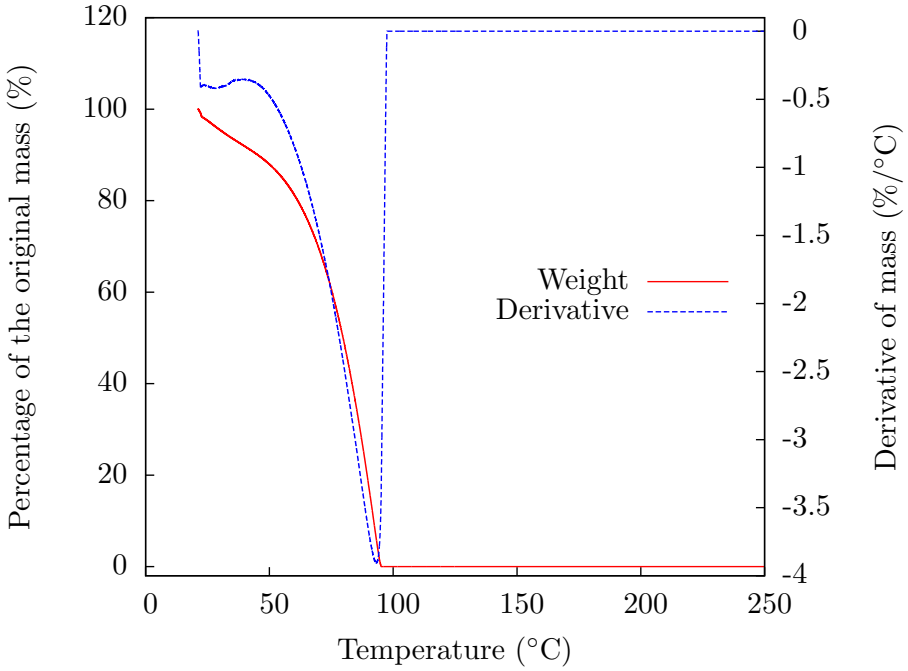

Figure 5.4: An example of the TGA of TMP.

The weight loss percentages shown by the TGA were converted into the corresponding molar masses using the formula

$$M_{\text{loss}} = M_{5\text{Calcium lactate}+n\text{TMP}} \times \%_{\text{loss}} \tag{5.2}$$

where n is the ratio of TMP (either 3, 12, 24 or 60).

5.3.1 Ratio of 5:3

The TGA of ratio 5:3 gave four weight losses at similar temperatures to calcium lactate; an example of this is shown in Figure 5.5. These percentage weight loss steps were converted into the molar masses shown in Table 5.4

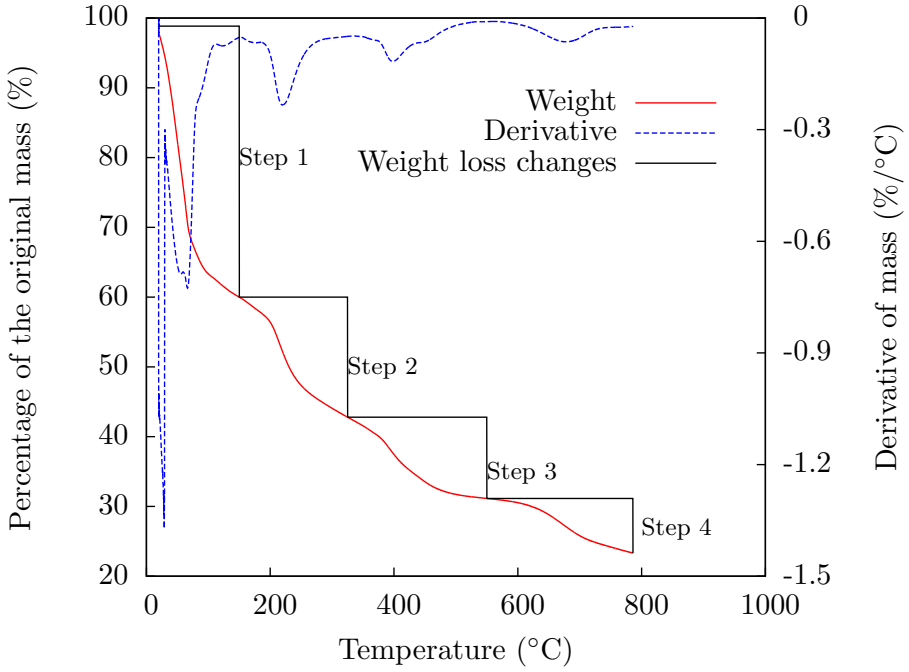

Figure 5.5: An average of the TGA of ratio 5:3.

Weight loss step	Temperature	Percentage	Molar mass
1^{st}	0-150°C	$39.24\% \pm 4.47\%$	$737.53\,\mathrm{gmol}^{-1}$
2^{nd}	151-325°C	$17.01\% \pm 3.63\%$	$319.76\,\mathrm{gmol}^{-1}$
3^{rd}	326-550°C	$11.93\% \pm 1.80\%$	$224.22\,\mathrm{gmol}^{-1}$
4^{th}	551-800°C	$8.04\% \pm 2.32\%$	$151.10\,\mathrm{gmol}^{-1}$
Final	800°C	$23.24\% \pm 3.82\%$	$436.85\,\mathrm{gmol}^{-1}$

Table 5.4: Conversion of percentage weight loss to molar mass using a ratio of 5 calcium lactates to 3 TMP.

As previously stated, if the calcium lactate and the TMP do not react, the final product from the TGA would be calcium oxide. The data for the final value shows there is a higher amount of mixture (23.24%±3.82%) left at the end of the TGA run than if it was solely calcium oxide (14.92%). This leads to three possibilities; the first is that the calcium lactate is not fully decomposing and there is some calcium carbonate still present. To get the remaining percentage within the errors, the ratio of calcium oxide to calcium carbonate could be 0:4 (26.63%), 1:4 (24.29%), 2:3 (21.94%) or 3:2 (19.60%). The second possibility is that the TMP reacts with the calcium lactate and the remaining product is a calcium phosphate compound. The third possibility is that both of these occur and that there is calcium carbonate, calcium oxide and calcium phosphate in the remaining product or it involves a carbonated calcium phosphate. The FTIR of the final product showed that it contained the same phosphate peaks as trimethyl phosphate and therefore there must be some calcium phosphate compound in the remaining product. EDS analysis of the product confirmed that there was phosphorus in the final product of the TGA. These results show that some TMP is reacting.

On comparing the FTIR analysis of the TGA sample to the FTIR of tricalcium phosphate ($Ca_3(PO_4)_2$), dibasic calcium phosphate ($CaHPO_4$) and HAp, we observe a resemblance to the dibasic calcium phosphate. The EDS data gave an elemental ratio of calcium, phosphorus, oxygen and carbon which was compared with that expected for dibasic calcium phosphate. From the EDS data and the FTIR spectra we conclude that the final product formed is likely to be dibasic calcium phosphate.

It is not clear exactly how the TMP and the calcium lactate react with one another. However, as TMP on its own is completely removed by 100°C, we infer that the reaction occurs at relatively low temperatures. The TMP could directly react with the calcium lactate. However, the reaction we believe could be occurring is a possible hydrolysis of the ester in which the methyl groups on the TMP molecule react with the water molecules attached to the calcium lactate to form methanol; these methanol molecules subsequently evaporate out at relatively low temperatures. Based on this, we assumed that a TMP molecule either reacts completely by losing all its methyl groups or it does not react with calcium lactate and is lost in the first step.

To form the desired HAp all three TMP molecules are needed to react with the calcium lactate. If only two TMP molecules react then the final product may be tricalcium phosphate, plus calcium oxide from the unreacted calcium lactate. If only one TMP molecule reacts, then it is predicted that dibasic calcium phosphate is formed, plus calcium oxide from the unreacted calcium lactate. To form any of these calcium phosphate products the TMP molecule must attach to the calcium lactate and lose water molecules. The number of water molecules lost depends on the final product formed; as we concluded that the final product is likely to be dibasic calcium phosphate, then only one water molecule is lost.

The FTIR spectra of the products formed from each weight loss step show that these are the same as the weight loss steps for calcium lactate but with phosphate peaks; see Table 5.5 for the calculated differences.

	Percentage
1^{st}	$39.24\% \pm 4.47\%$
2TMP	14.91%
$17.5H_2O$	16.77%
$3CH_3OH$	5.11%
Difference	2.45%
2^{nd}	$17.01\% \pm 3.63\%$
$2H_2O$	9.59%
H_2O	0.96%
Difference	6.47%
3^{rd}	$11.93\% \pm 1.80\%$
C_5H_6O	21.84%
Difference	-9.91%
4^{th}	$8.04\% \pm 2.32\%$
CO_2	11.71%
Difference	-3.67%
Final weight	$23.24\% \pm 3.82\%$
$CaHPO_4$	36.20%
Difference	-12.95%

Table 5.5: The predicted overall decomposition of 5:3: the experimental weight loss of each step, weight loss of the predicted compound(s) and the difference between the two.

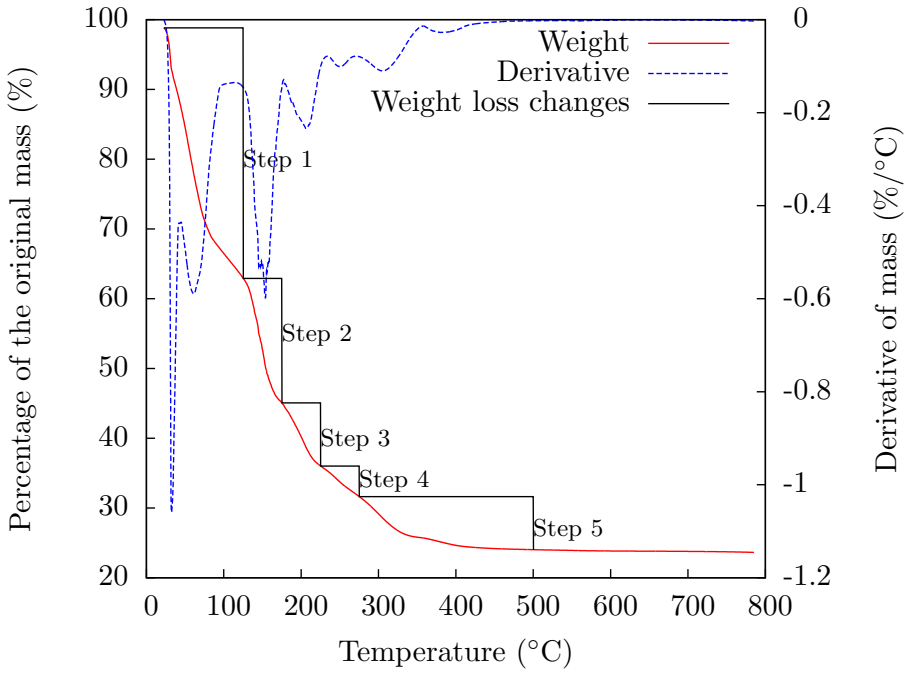

Figure 5.6: An average of the TGA of ratio 5:12.

5.3.2 Ratio of 5:12

Using an excess of TMP, there is a higher chance of the calcium lactate reacting with the TMP to form a calcium phosphate product. Figure 5.6 shows the percentage weight loss steps for a ratio of 5:12; these losses are given in Table 5.6.

The final product formed was not calcium oxide as the percentage weight remaining after TGA (23.83%) was larger than that of calcium oxide (8.93%). It was also larger than if solely calcium carbonate was formed (15.94%). The FTIR and EDS analyses of the final product showed that there is phosphate present in the remaining product. The FTIR of the resulting product shows that it is a calcium phosphate compound. From comparing it to the FTIR of calcium phosphate compounds, it could be either tricalcium phosphate or HAp. From the EDS data

Weight loss step	Temperature	Percentage	Molar mass
1^{st}	0-125°C	$35.03\% \pm 10.28\%$	$1100.12\,\mathrm{gmol}^{-1}$
2^{nd}	126-175°C	$18.57\% \pm 6.26\%$	$583.00\,\mathrm{gmol}^{-1}$
3^{rd}	176-225°C	$9.29\% \pm 0.17\%$	$291.75\,\mathrm{gmol}^{-1}$
4^{th}	226-275°C	$4.55\pm1.04\%$	$143.02\,\mathrm{gmol}^{-1}$
5^{th}	276-500°C	$7.94\% \pm 0.28\%$	$249.33\,\mathrm{gmol}^{-1}$
Final	500°C	$23.83\% \pm 1.85\%$	$748.36\,\mathrm{gmol}^{-1}$

Table 5.6: Conversion of percentage weight loss to molar mass using a ratio of 5 calcium lactates to 12 TMP.

we infer that the product is likely to be tricalcium phosphate.

The first weight loss step (35.03%±10.28%) of the mixture also indicates that calcium lactate and TMP are reacting, as it is lower than expected if no reaction occurs. Therefore, it is believed that some of the water and/or TMP are retained in the sample as they react and form other compounds. Continuing on the idea that methanol is being formed as a by-product from the reaction, a maximum of 18 methanol molecules could be formed. There are 20.5 water molecules available to react with the methyl groups on the TMP; using the same assumption as before, that the TMP either completely reacts or it does not at all, a maximum of 18 water molecules will react with six TMP molecules. This would leave 2.5 water molecules, six TMP molecules and 18 methanol molecules to be removed in the first weight loss (46.57%). This is not within the error of the weight loss step. However, this difference is made up for in the second weight loss step difference. The reaction of six TMP can cause more than one type of calcium phosphate compound to be formed, due to this the number of water molecules lost from the TMP is unknown.

The big difference with ratio of 5:12 is that there are five weight loss steps, as

shown in Figure 5.6. This makes it look complicated but it could be due to the third step (9.29%) being smaller than expected if C_5H_6O (13.07%) was lost and the loss of carbon dioxide (7.01%) being consistent with the fifth weight loss step (7.94%). This suggests that the extra weight loss step is caused by the third weight loss step being the loss of C_4H_6 (8.61%) and the fourth weight loss step (4.55%) being the loss of carbon monoxide (4.46%). The second weight loss (18.57%) is too large to be just the loss of structural water molecules from the calcium lactate and the TMP. As the temperature of the second weight loss step for 5:12 (175°C) is so much lower than for 5:3 (225°C), the methanol formed could be lost in the second weight loss step rather than the first.

The FTIR spectra of the other weight loss steps are similar to the weight loss steps of ratio 5:3 except the phosphate peaks are bigger. The overall predicted decomposition is shown in Table 5.7.

5.3.3 Ratio of 5:24

The TGA of the ratio of 5:24 only shows four weight loss steps (see Figure 5.7). However, from looking at the 5:12 ratio, it was believed that the third weight loss step contained the loss of C_4H_6 and carbon monoxide. These percentage weight loss steps were converted into molar mass, shown in Table 5.8.

In a mixture of 5:24, the results suggest the same mechanism is happening as in 5:12. The final product is a calcium phosphate compound. The FTIR spectra for the resulting product shows that it could be either tricalcium phosphate or HAp. However, from the EDS data we infer that HAp may be produced. The

	Percentage
1^{st}	$35.03\% \pm 10.28\%$
6TMP	26.76%
$2.5H_2O$	1.43%
$18CH_3OH$	18.37%
Difference	-11.73%
2^{nd}	$18.57\% \pm 6.26\%$
$10H_2O$	5.74%
$?H_2O$	unknown
Difference	12.83%
3^{rd}	$9.29\% \pm 0.17\%$
C_4H_6	8.61%
Difference	0.68%
4^{th}	$4.55 \pm 1.04\%$
CO	4.46%
Difference	0.09%
5^{th}	$7.94\% \pm 0.28\%$
CO_2	7.01%
Difference	0.93%
Final weight	$23.83\% \pm 1.85\%$
$Ca_3(H_2PO_4)_2$	9.88%
Difference	12.65%

Table 5.7: The predicted overall decomposition of 5:12: the experimental weight loss of each step, weight loss of the predicted compound and the difference between the two.

Weight loss step	**Temperature**	**Percentage**	**Molar mass**
1^{st}	0-125°C	$41.26\% \pm 19.03\%$	$1988.97\,\mathrm{gmol}^{-1}$
2^{nd}	126-175°C	$27.54\% \pm 13.63\%$	$1327.91\,\mathrm{gmol}^{-1}$
3^{rd}	176-225°C	$7.01\% \pm 5.23\%$	$337.72\mathrm{mol}^{-1}$
4^{th}	226-400°C	$5.89\% \pm 2.09\%$	$283.93\,\mathrm{gmol}^{-1}$
Final	400°C	$17.29\% \pm 3.43\%$	$833.46\,\mathrm{gmol}^{-1}$

Table 5.8: Conversion of percentage weight loss to molar mass using a ratio of 5 calcium lactates to 24 TMP.

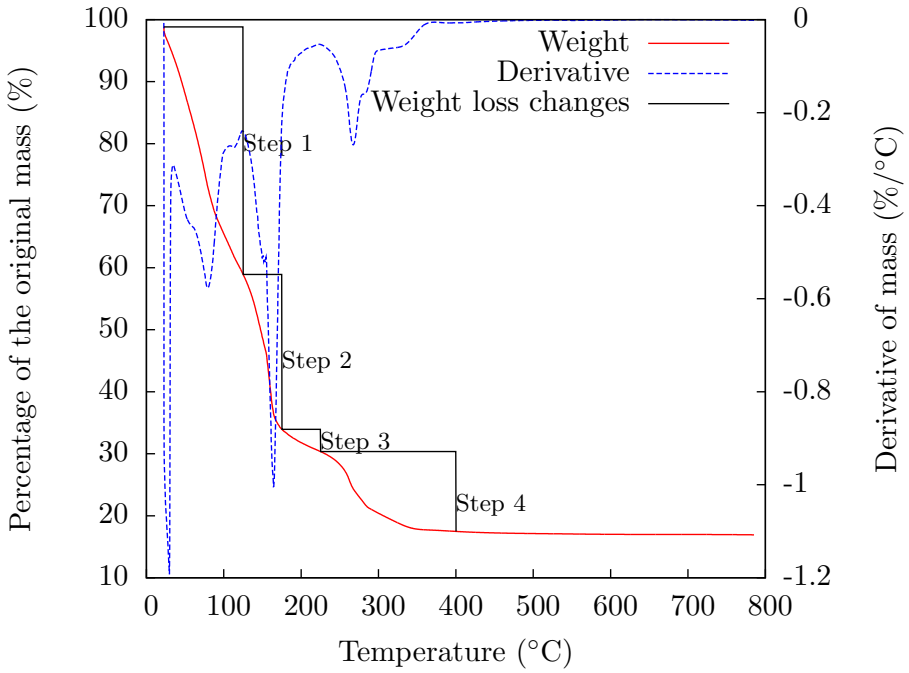

Figure 5.7: An average of the TGA of ratio 5:24.

first weight loss step (41.26%±19.03%) indicates how many TMP molecules are reacting with calcium lactate. As in the ratio of 5:12, the maximum number of TMP which can react is six. This gives a calculated weight loss of 53.23%, which is within the errors of this step. Therefore, more than one calcium phosphate compound could be being formed; again this means that the number of water molecules lost from the TMP is unknown.

All the other weight loss steps show that the same decomposition of the calcium lactate and the TMP occur. This is shown in Table 5.9.

	Percentage
1^{st}	$41.26\% \pm 19.03\%$
6TMP	52.30%
$2.5H_2O$	0.93%
Difference	-11.98%
2^{nd}	$27.54\% \pm 13.63\%$
$18CH_3OH$	11.96%
$10H_2O$	3.74%
$?H_2O$	unknown
Difference	11.84%
3^{rd}	$7.01\% \pm 5.23\%$
C_4H_6	5.61%
CO	2.90%
Difference	-1.51%
5^{th}	$5.89\% \pm 2.09\%$
CO_2	4.56%
Difference	1.33%
Final weight	$17.29\% \pm 3.43\%$
$Ca_5(PO_4)_3OH$	10.42%
Difference	6.87%

Table 5.9: The predicted overall decomposition of 5:24: the experimental weight loss of each step, weight loss of the predicted compound(s) and the difference between the two.

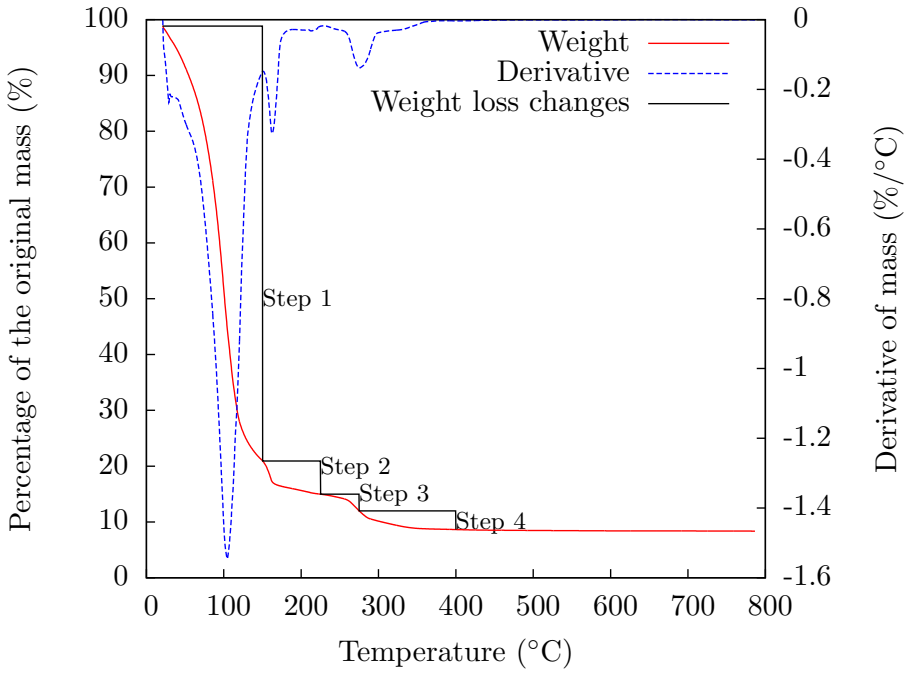

Figure 5.8: An average of the TGA of ratio 5:60.

5.3.4 Ratio of 5:60

A very large excess of TMP was tested (5:60). This showed four weight loss steps, as seen in Figure 5.8, which were converted into molar mass, shown in Table 5.10.

The calculated TGA data showed the same breakdown of the compounds ending

Weight loss step	Temperature	Percentage	Molar mass
1^{st}	0-150°C	78.26%±5.66%	7719.40 $gmol^{-1}$
2^{nd}	151-225°C	6.33%±2.96%	623.95 $gmol^{-1}$
3^{rd}	226-275°C	4.84%±2.41%	477.82 $gmol^{-1}$
4^{th}	276-400°C	1.66%±0.21%	163.67 $gmol^{-1}$
Final	400°C	8.48%±1.03%	836.88 $gmol^{-1}$

Table 5.10: Conversion of percentage weight loss to molar mass using a ratio of 5 calcium lactates to 60 TMP.

in a calcium phosphate compound. The FTIR spectra shows that a calcium phosphate product is remaining; we conclude from the EDS data that the product is likely to be HAp. As with the 5:12 and 5:24 ratios, the first weight loss step (78.26%±5.66%) shows how many TMP could be reacting. Out of the calculated weight loss data it suggests that three to six TMP are reacting with the calcium lactate and therefore, more than one type of calcium phosphate product is being formed.

5.4 Conclusion

Calcium lactate and TMP react to form a calcium phosphate compound. Using a sufficient excess of TMP (at least a ratio of 5:24) will make sure that HAp can be produced and not just tricalcium phosphate or dibasic calcium phosphate. Using an excess of TMP showed that TMP prefers to react with calcium lactate if there is enough available to do so. Assuming that the PP-MOCVD precursors behave in a similar manner when decomposing in the reaction chamber, then an excess of TMP should be used in the precursors.

Another important feature shown by these TGA experiments is that with an excess of TMP (5:24 or 5:60), the entire decomposition of the precursor is complete at a lower temperature (400°C) and did not need to be heated up to 800°C as required for the lower ratios. Therefore, the substrate deposition temperature required for the PP-MOCVD in order to form the calcium phosphate compound on the substrate surface is at least 400°C. However, a higher temperature may be required in PP-MOCVD as there is less heating time than in the TGA.

Use of an excess of TMP in the ratio of 5:60 is not necessary as 5:24 gave similar results.

Chapter 6

PP-MOCVD RESULTS

The pulse pressure metal organic chemical vapour deposition (PP-MOCVD) system was first developed at Cornell University in 1993 and then brought to the University of Canterbury in 2000.[44] This system can be used to form a range of thin films using many different precursors due to its simplicity of operation and the relative ease of control of the deposition process, plus the ability to adjust and control many parameters of the system.

In this study a number of parameters were looked at: substrate deposition temperature, ratio of components in the precursor solution, annealing for various times and temperatures, the number of pulses, concentration of precursor solution, the effect of substrate heating and using a dry precursor. The ideal surface would have a thin uniform coating of HAp. All surfaces were analysed by colour observation, FTIR, SEM and EDS.

Ratio	Deposition temperature		
	400°C	**500°C**	**600°C**
5:6	68**Ca**:3**P**:217**O**:165**C**	13**Ca**:3**P**:57**O**:47**C**	11**Ca**:3**P**:59**O**:26**C**
5:18	60**Ca**:3**P**:194**O**:177**C**	8**Ca**:3**P**:56**O**:32**C**	6**Ca**:3**P**:17**O**:31**C**

Table 6.1: Ratio of elements observed by EDS for varying deposition temperatures.

6.1 Deposition temperature

The TGA study showed that the temperature resulting in the entire decomposition of the precursor containing excess TMP was 400°C. This implies that the PP-MOCVD substrate deposition temperature needs to be at least 400°C, assuming that the precursor decomposes in the same manner in the PP-MOCVD. However, the TGA and PP-MOCVD equipment operate under different conditions; in PP-MOCVD the precursor solution is sprayed towards the heated substrate under vacuum, while in TGA the precursor mixture is placed within a furnace chamber under nitrogen. Three deposition temperatures (400°C, 500°C and 600°C) were tested for two solution ratios of calcium lactate to TMP (5:6 and 5:18). 999 pulses were used, each containing 100μL of a 0.15 mole% calcium lactate precursor solution at room temperature.

The SEM images show that these surfaces are not uniformly smooth on the micro-scale. However, the uniformity does increase with increased deposition temperature, as shown by Figure 6.1. The EDS data, given in Table 6.1, showed that none of the surface coatings had element ratios consistent with pure HAp ($Ca_5P_3O_{13}H$). All of them have a significant carbon contamination. This contamination is presumably due to the precursor and/or the solvent not entirely decomposing, leaving a carbonated calcium phosphate coating. This would also

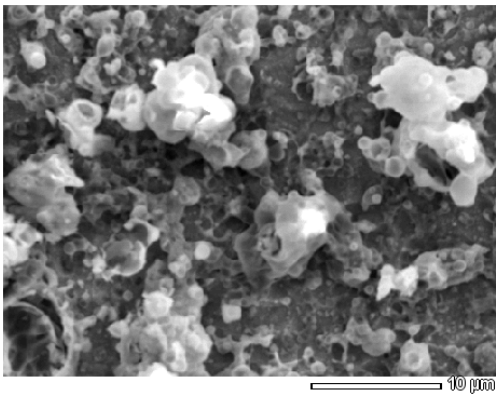

(a) 400°C

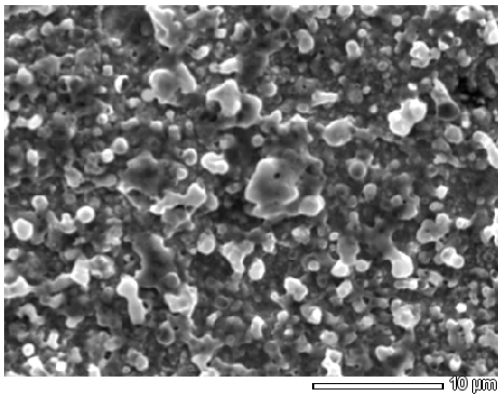

(b) 500°C

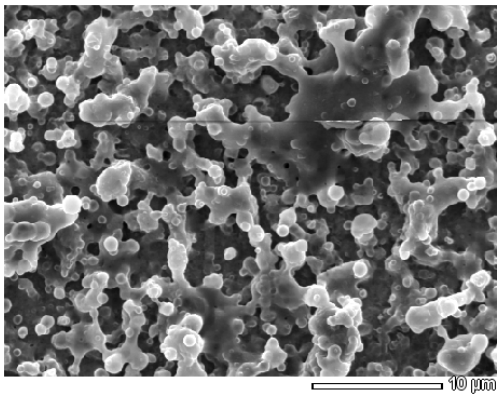

(c) 600°C

Figure 6.1: SEM images of titanium substrates with coatings formed from a 5:6 ratio at varying deposition temperatures.

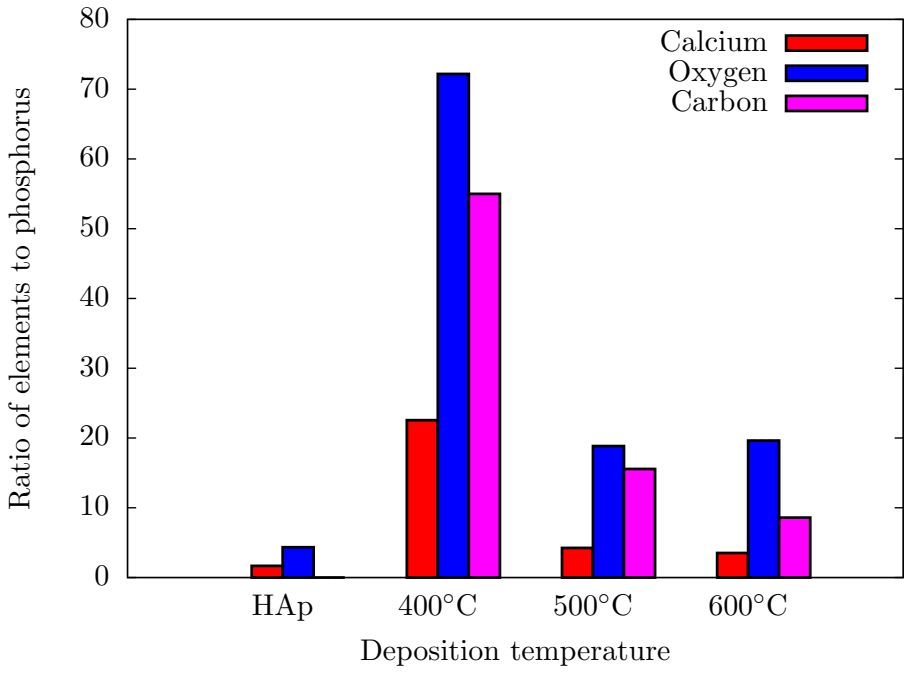

(a) 5:6

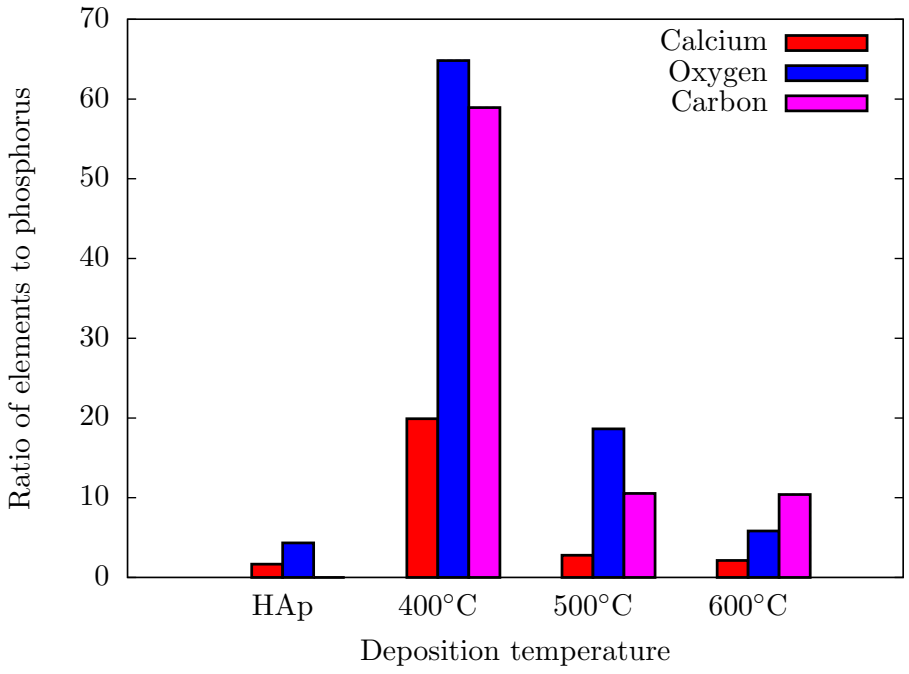

(b) 5:18

Figure 6.2: Ratio of elements to phosphorus on the surface of the substrate for different deposition temperatures. The ratio of HAp is given for comparison.

explain why there is more oxygen present than that found in HAp. The amount of calcium remaining in the 5:6 coatings is also higher than expected, which could be due to not enough TMP reacting with the calcium lactate as the amount of calcium does decrease as the ratio of TMP increases. Increasing the deposition temperature has decreased the amount of calcium, oxygen and carbon with respect to phosphorus, as seen in Figure 6.2. It would be logical to use a higher deposition temperature to get a better result. However, using a hotter temperature can reduce the lifespan of the heater. As a compromise the remaining tests were conducted with a deposition temperature of 500°C.

6.2 Ratio of calcium lactate to TMP

If there is insufficient TMP present, the calcium lactate will decompose to form calcium oxide or react with what TMP there is and form tricalcium phosphate or dibasic calcium phosphate instead of HAp. This was looked at in the TGA study; however, the differing conditions of the TGA and PP-MOCVD may result in the calcium lactate and TMP reacting differently during deposition. To check this, PP-MOCVD runs were performed using a calcium to phosphate ratio the same as the stoichiometry of HAp (5:3) and using excess amounts of TMP (5:6, 5:12, 5:18, 5:24 and 5:30). Each solution was at a concentration of 0.15 mole% of caclium lactate and kept at room temperature. 999 pulses were performed at a deposition temperature of 500°C.

The SEM images of Figure 6.4 show that the coating is not uniform. However, there is a slight increase in coating coverage when a larger amount of TMP is

Ratio of calcium lactate to TMP	
5:3	79**Ca**:3**P**:288**O**:243**C**
5:6	13**Ca**:3**P**:56**O**:47**C**
5:12	11**Ca**:3**P**:40**O**:31**C**
5:18	7**Ca**:3**P**:41**O**:24**C**
5:24	6**Ca**:3**P**:17**O**:13**C**
5:30	5**Ca**:3**P**:14**O**:47**C**

Table 6.2: Ratio of elements observed by EDS for varying precursor ratios.

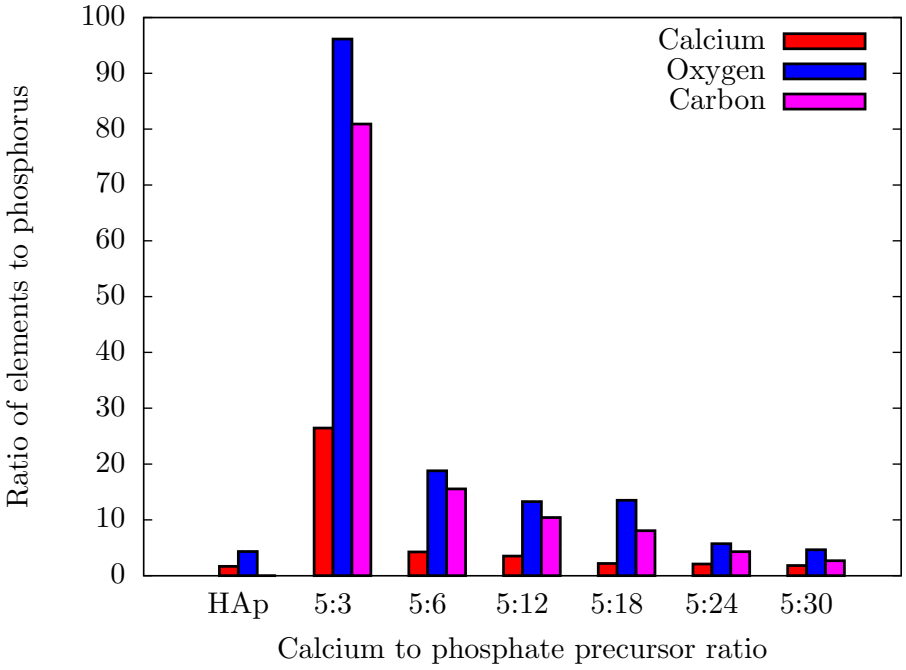

Figure 6.3: Ratio of elements to phosphorus on the surface of the substrate for different precursor ratios. The ratio of HAp is given for comparison.

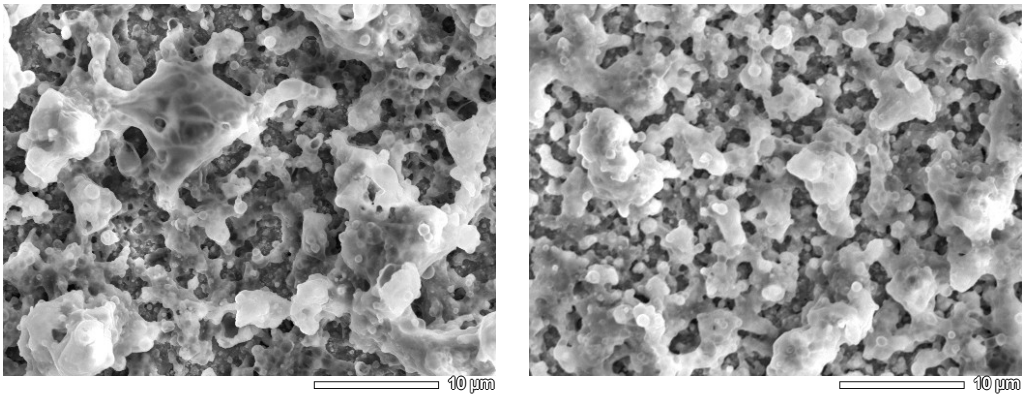

(a) 5:3 (b) 5:24

Figure 6.4: SEM images of a coated titanium substrates at different precursor ratios of calcium lactate to TMP.

used. The EDS data, given in Table 6.2 and Figure 6.3, show that none of the coatings are pure HAp as they all contain carbon contaminants. However, as the amount of TMP increases, the difference between the abundance of these elements decreases. A ratio of 5:30 gave the correct ratio of calcium to phosphate on the surface. However, to be consistent with the TGA studies the ratio of 5:24 was used for the majority of the remaining experiments.

6.3 Annealing

Annealing is a heat treatment method where a material is altered; for example, it can remove contaminants and improve the homogeneity of the material. Other studies of HAp coatings have used annealing, which has had a great influence on the final coating properties.[60] There are reports of the conversion of the amorphous HAp to the crystalline phase, resulting in a uniform coating.[61] The calcium to phosphate ratio decreased as the annealing temperature increased. However,

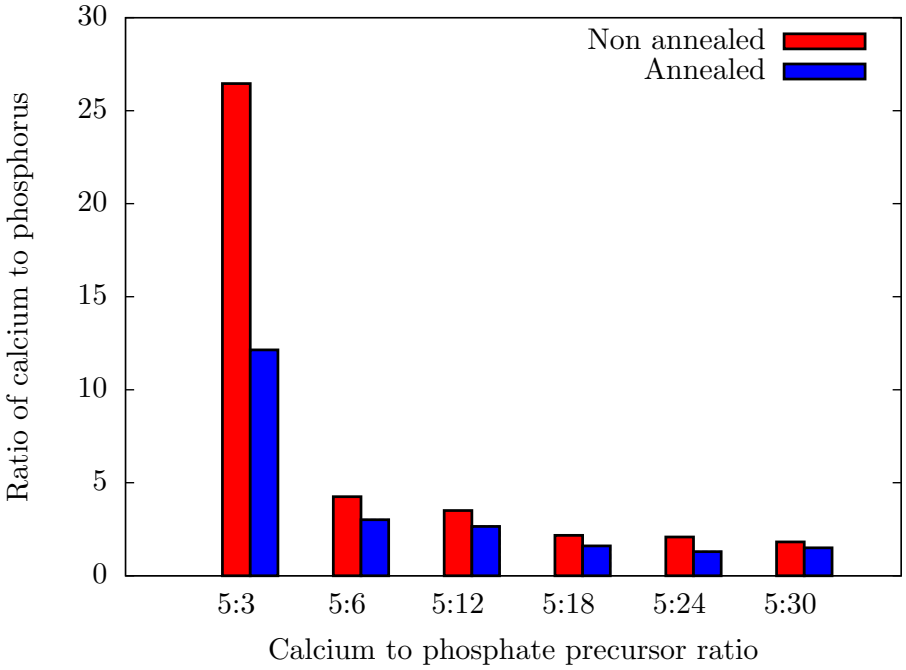

Figure 6.5: The ratio of calcium to phosphorus with and without substrate annealing for one hour at 100 Pa.

if the temperature was 800°C or above, the coating would be predominantly titanium dioxide (TiO_2).[62]

In this research two methods of annealing were tested, the first being at a pressure of 100 Pa and the second being at atmospheric pressure.

6.3.1 100 Pa pressure

This method was performed by leaving the substrate in the PP-MOCVD apparatus for one hour at 500°C after the pulsing had finished. This was performed at a number of different precursor ratios (5:3, 5:6, 5:12, 5:18, 5:24 and 5:30), using 999 pulses and precursor solutions of 0.15 mole%.

Ratio of calcium lactate to TMP	Non heated	Annealed
5:3	79**Ca**:3**P**:288**O**:243**C**	36**Ca**:3**P**:155**O**:53**C**
5:6	13**Ca**:3**P**:56**O**:47**C**	9**Ca**:3**P**:52**O**:29**C**
5:12	11**Ca**:3**P**:40**O**:31**C**	8**Ca**:3**P**:13**O**:8**C**
5:18	7**Ca**:3**P**:41**O**:24**C**	5**Ca**:3**P**:18**O**:15**C**
5:24	6**Ca**:3**P**:17**O**:13**C**	4**Ca**:3**P**:27**O**:17**C**
5:30	5**Ca**:3**P**:14**O**:47**C**	5**Ca**:3**P**:19**O**:9**C**

Table 6.3: Ratio of elements observed by EDS for varying precursor ratios with or without annealing for one hour at 100 Pa.

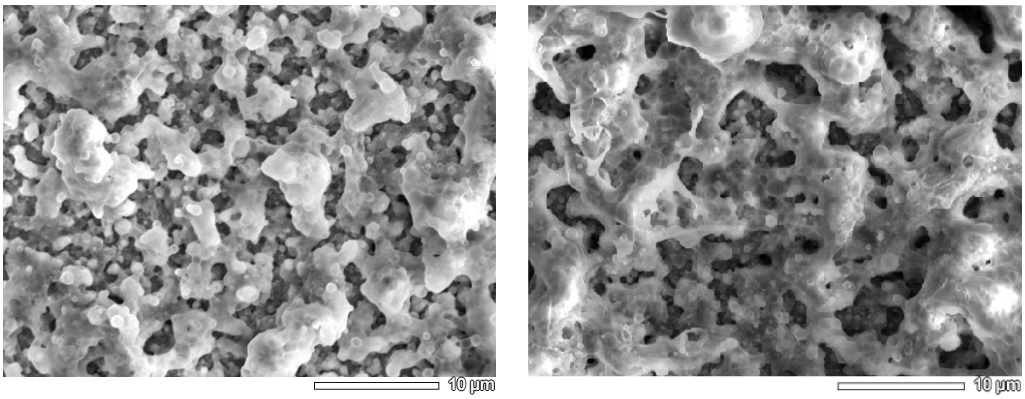

(a) (b)

Figure 6.6: SEM images of a titanium substrate coated with a precursor solution of 5:24 (a) without annealing and (b) with annealing.

As shown in Figure 6.5 annealing does improve the ratio of calcium to phosphorus. The EDS results are given in Table 6.3; these show that carbon contaminants are still present. The SEM images show that the coatings are not uniform, but there is an improvement on the annealed coating in Figure 6.6.

This method of annealing was then performed for various lengths of time (one, two, three and four hours). Based on the SEM images, given in Figure 6.7, longer annealing times did not form uniform coatings. However, it did reduce the size of the lumps on the substrate. The EDS data of Table 6.4 shows that there are

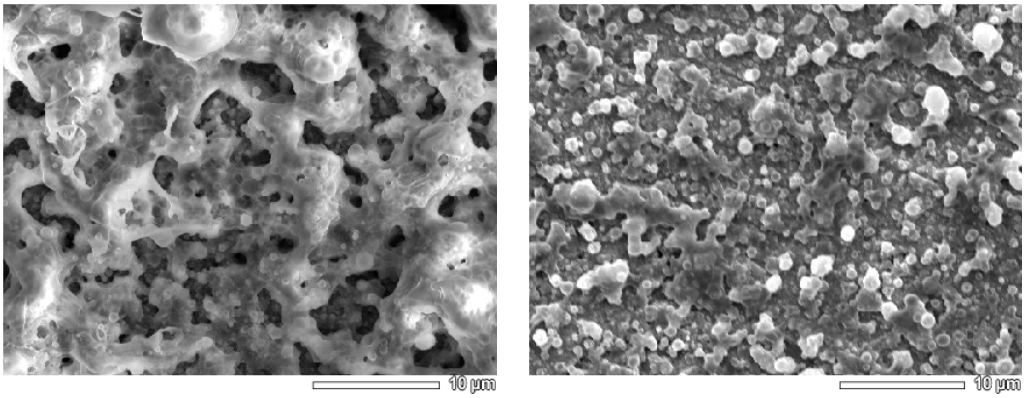

(a) (b)

Figure 6.7: SEM images of a titanium substrates coated with a precursor solution of 5:24 (a) with 1 hour of annealing and (b) with 4 hours of annealing.

Temperature	**Ratio**
Non heated	6**Ca**:3**P**:17**O**:13**C**
1hr	4**Ca**:3**P**:27**O**:17**C**
2hrs	3**Ca**:3**P**:30**O**:9**C**
3hrs	3**Ca**:3**P**:27**O**:8**C**
4hrs	3**Ca**:3**P**:28**O**:10**C**

Table 6.4: Ratio of elements observed by EDS for a 5:24 precursor ratio.

still carbon contaminants present and none of the annealing times tested gave the desired element ratios. Annealing for the first two hours showed that the ratio of calcium to phosphorus was reducing. However, longer times made little difference, as illustrated in Figure 6.8.

6.3.2 Atmospheric pressure

This method allows the use of hotter annealing temperatures as the temperature is not restricted by the PP-MOCVD heater. Each substrate was put into a kiln at different temperatures (500°C–1000°C at 100°C increments) for different times

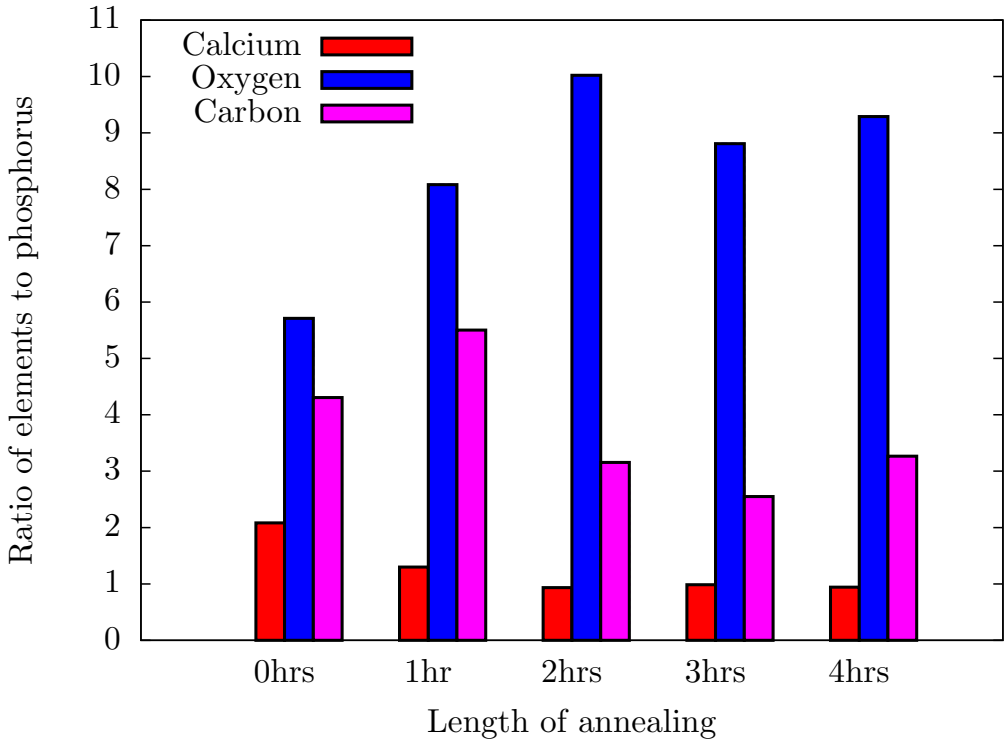

Figure 6.8: Ratio of elements to phosphorus on the surface of the substrate for different 100 Pa annealing times.

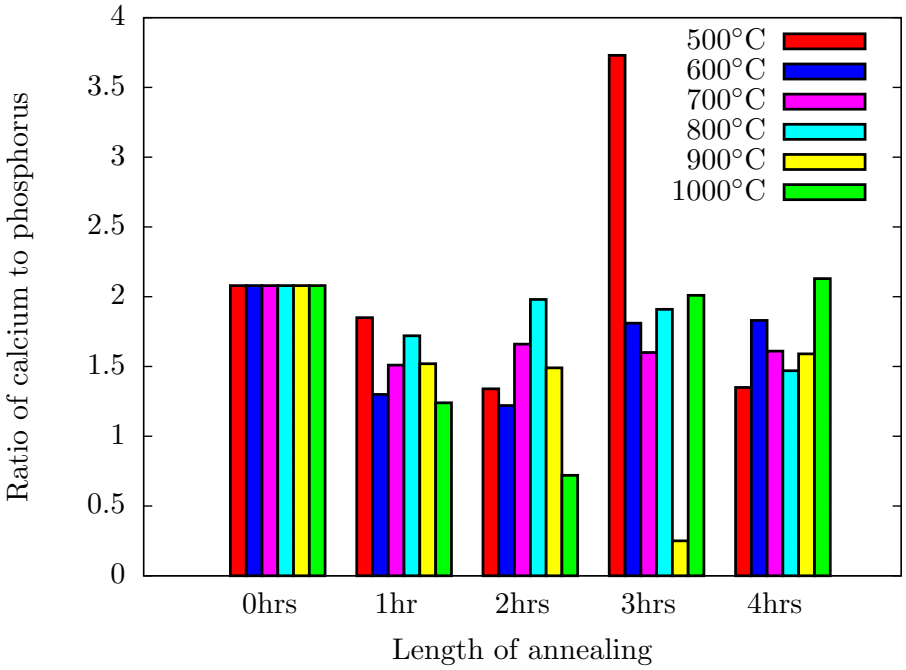

Figure 6.9: Ratio of calcium to phosphorus on the surface of the substrate for different atmospheric annealing times.

(one, two, three and four hours). All other variables were the same as for 100 Pa pressure annealing.

The longer the substrates were heated the lighter the coatings became. When looking at the substrate a colour change was observed as the length of annealing increased; for example, annealing at 1000°C, it went from dark grey to light grey to white and then pale yellow. This shows that the annealing is affecting the coating properties. The EDS data, given in Table 6.5, show that there are no trends in the calcium or carbon to phosphorus ratios; the calcium ratio is illustrated in Figure 6.9. However, some of the longer times and higher temperatures reduced or removed the carbon contamination. Another important feature that is shown by the EDS is that there is less coating on the substrate as annealing tem-

Temp	Non heated	1hr	2hrs
500°C	6**Ca**:3**P**:17**O**:13**C**	6**Ca**:3**P**:17**O**:27**C**	4**Ca**:3**P**:39**O**:4**C**
600°C	6**Ca**:3**P**:17**O**:13**C**	4**Ca**:3**P**:63**O**:2**C**	4**Ca**:3**P**:96**O**:0**C**
700°C	6**Ca**:3**P**:17**O**:13**C**	5**Ca**:3**P**:42**O**:2**C**	5**Ca**:3**P**:38**O**:0**C**
800°C	6**Ca**:3**P**:17**O**:13**C**	5**Ca**:3**P**:66**O**:2**C**	6**Ca**:3**P**:54**O**:0**C**
900°C	6**Ca**:3**P**:17**O**:13**C**	5**Ca**:3**P**:33**O**:1**C**	4**Ca**:3**P**:39**O**:1**C**
1000°C	6**Ca**:3**P**:17**O**:13**C**	4**Ca**:3**P**:79**O**:1**C**	2**Ca**:3**P**:145**O**:0**C**

Temp	3hrs	4hrs
500°C	4**Ca**:3**P**:44**O**:4**C**	4**Ca**:3**P**:37**O**:5**C**
600°C	5**Ca**:3**P**:36**O**:4**C**	5**Ca**:3**P**:33**O**:3**C**
700°C	5**Ca**:3**P**:421:4**C**	5**Ca**:3**P**:38**O**:2**C**
800°C	6**Ca**:3**P**:93**O**:1**C**	4**Ca**:3**P**:163**O**:0**C**
900°C	1**Ca**:3**P**:1142**O**:5**C**	5**Ca**:3**P**:1537**O**:0**C**
1000°C	6**Ca**:3**P**:1125**O**:9**C**	6**Ca**:3**P**:1670**O**:87**C**

Table 6.5: Ratio of elements observed by EDS for varying atmospheric annealing times and temperatures.

peratures and times increased, as seen in Table 6.6. In a perfect coating of HAp, ignoring the hydrogen as the EDS does not measure hydrogen, there would be 38% calcium plus phosphorus and minimal amount of titanium showing. Figure 6.10 shows that the hotter the annealing temperature or the longer the substrate is annealed, the less calcium and phosphorus is present. Instead the substrate forms TiO_2; this also explains the significant increase in oxygen to phosphate ratio, which is consistent with the findings of Boyd *et al.*[62] Figure 6.11 shows the visible differences between the coatings as the annealing temperatures increase.

Overall gentle annealing has proven to help with the ratio of the elements present to make them more like HAp and helped with the uniformity of the coating. However, vigorous annealing removes the coating from the substrate and results in the formation of TiO_2. Using an annealing temperature of 700°C gives a ratio of calcium to phosphate the same as HAp; additionally it is more uniform than

Temp	1hr	2hrs	3hrs	4hrs
500°C	15.29%	10.51%	7.34%	11.74%
600°C	5.39%	17.03%	12.71%	12.97%
700°C	8.57%	13.11%	11.20%	11.85%
800°C	12.04%	8.78%	7.09%	3.46%
900°C	11.20%	13.39%	0.37%	0.20%
1000°C	3.68%	0.94%	0.23%	0.50%

Table 6.6: Percentage of surface area covered by calcium plus phosphorous in each of the coatings, observed by EDS, at different atmospheric annealing times and temperatures.

the lower temperatures, the surface has an ideal amount of calcium phosphorus coating and is not just TiO_2.

6.4 Number of pulses

The number of pulses used is important as it controls the thickness of the coating. Forming a thick coating runs the risk of it scratching off. In the general sense of this research, this would increase the risk of parts of the coating getting into the blood stream, which could cause medical problems for the patient. This would also slow down the rate of bone in-growth which would cause the patient a longer and more painful recovery time. Forming a very thin coating can also slow down bone in-growth, as there is less coating to bind to. Additionally, it is harder to analyse a very thin coating, as the data is weak. An ideal middle ground is required for the purpose of this research.

Using 999 pulses caused the coating to be very thick and easily scratched off. To test different thicknesses the number of pulses were varied. The precursor solution was in a ratio of 5:24 and a concentration of 0.15 mole%. The coatings

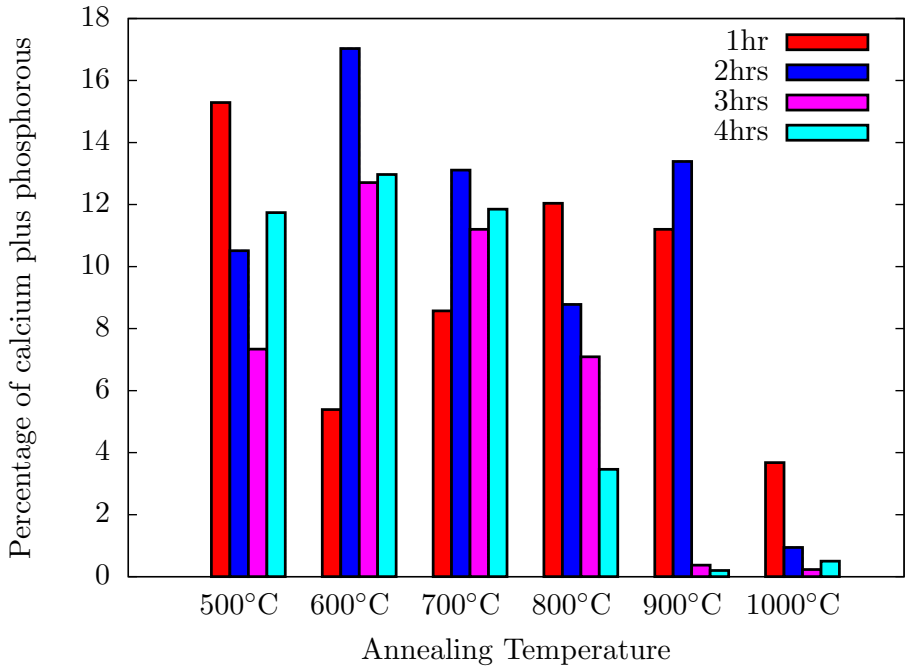

Figure 6.10: Percentage of surface area covered by calcium and phosphorous in each of the coatings using atmospheric annealing at different temperatures and times.

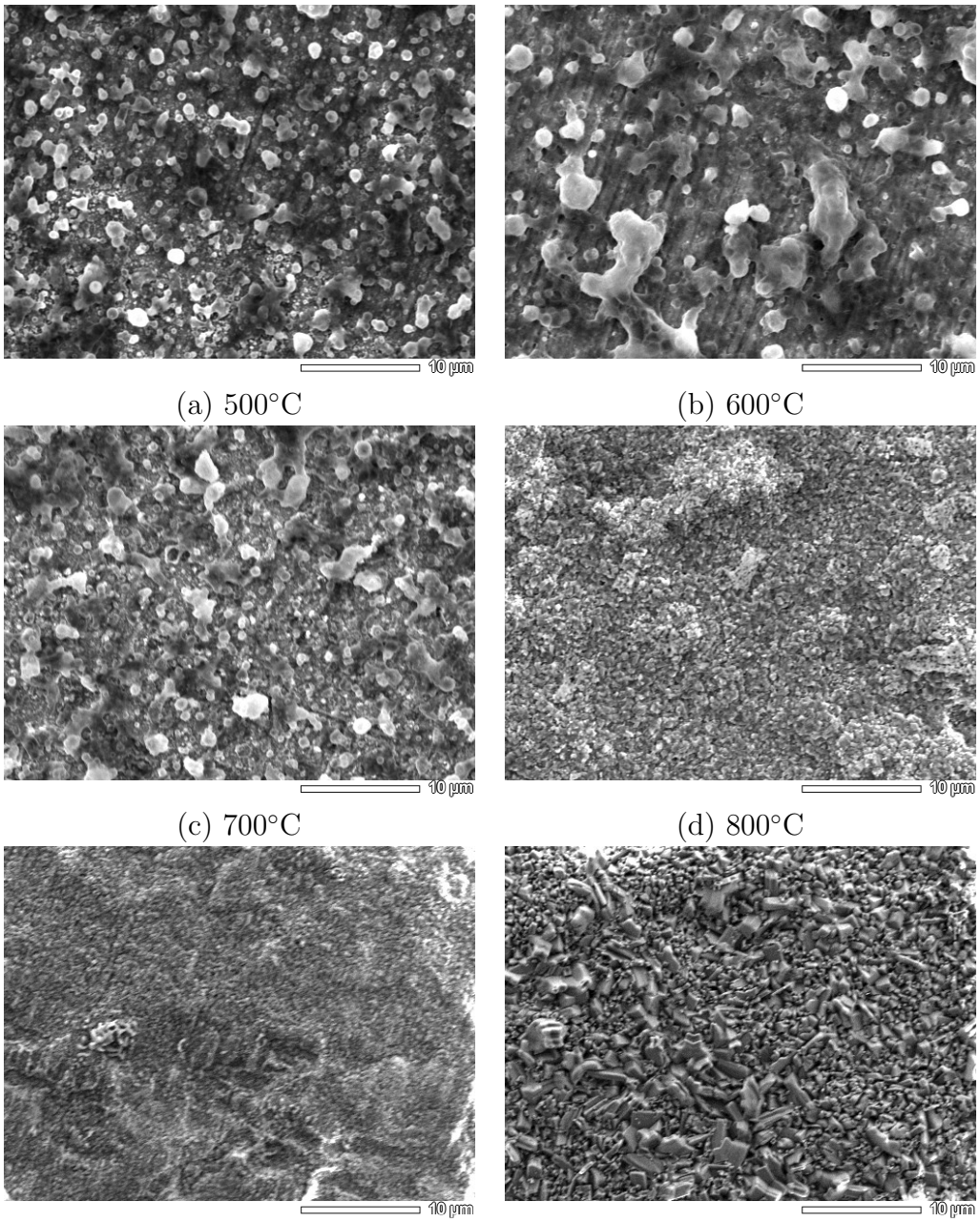

(a) 500°C (b) 600°C

(c) 700°C (d) 800°C

(e) 900°C (f) 1000°C

Figure 6.11: SEM images of titanium substrates coated with a precursor solution of 5:24 after 4 hours of atmospheric annealing.

Number of pulses	
100	2**Ca**:3**P**:19**O**:91**C**
200	3**Ca**:3**P**:16**O**:35**C**
400	6**Ca**:3**P**:15**O**:55**C**
600	4**Ca**:3**P**:27**O**:50**C**
800	3**Ca**:3**P**:13**O**:20**C**
999	4**Ca**:3**P**:17**O**:27**C**

Table 6.7: Ratio of elements observed by EDS for varying number of pulses with 1 hour of 100 Pa annealing. This had a precursor ratio of 5:24.

were annealed at 500°C for one hour using the 100 Pa method and the ratios were checked by EDS to make sure that they were not affected; this data is given in Table 6.7.

All the substrates could easily be scratched with a pair of tweezers. In future tests 400 pulses were used as it was thick enough to be easily analysed, it did not scratch as badly as the thicker coatings, it would take less time to perform the run and also the ratio of calcium to phosphorus was closest to hydroxyapatite.

6.5 Precursor concentration

As the previous coatings were not uniform and there was a white precipitate on the reaction chamber wall, it was considered that the precursor concentration was too high. Therefore, a range of concentrations (0.150 mole%, 0.075 mole%, 0.038 mole%, 0.018 mole% and 0.009 mole%) were tested. When trying to form a coating with a particular number of moles of precursor, the concentration and the number of pulses are inversely proportional to each other. To ensure that the coatings had the same amount of calcium and phosphorous present the number of

Concentration	
0.150 mole%	2**Ca**:3**P**:38**O**:7**C**
0.075 mole%	2**Ca**:3**P**:48**O**:7**C**
0.038 mole%	3**Ca**:3**P**:39**O**:9**C**
0.018 mole%	3**Ca**:3**P**:176**O**:5**C**
0.009 mole%	2**Ca**:3**P**:31**O**:8**C**

Table 6.8: Ratio of elements observed by EDS for different concentrations.

pulses used were 150, 300, 600, 1200 and 2400 respectively. The other variables were the same as the above experiment, except that no annealing was performed.

These experiments were performed with a black background behind the reaction chamber, so that the precipitate could be seen more clearly. Photos of the precipitate were taken to be compared against each other. The photos showed that the precipitate was the same over all the precursor concentrations.

The EDS values shown in Table 6.8 confirmed that approximately the same ratio of elements was present. Therefore, the number of pulses were correctly set to give the same amount of precursor. However, the amount of calcium to phosphorus present is low; the reason for this is unknown. The SEM images, given in Figure 6.12 show that the coating is unchanged with different precursor concentrations.

6.6 Ambient tests

Another possible reason for the non-uniform coating and the deposit on the reaction chamber is that the precursor solution is not vapourising and decomposing. Instead the calcium lactate and TMP could be reacting with each other and would

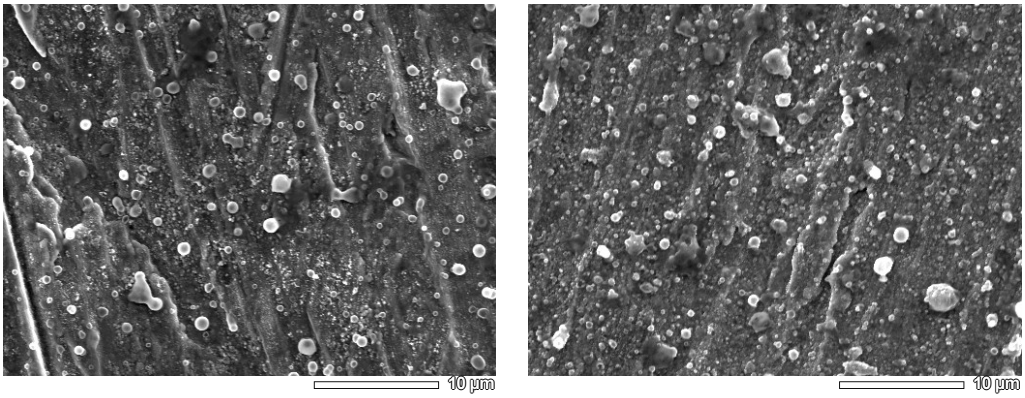

(a) (b)

Figure 6.12: SEM images of titanium substrates coated with a precursor solution of 5:24 at (a) 0.15 mole%, 150 pulses and (b) 0.009 mole%, 2400 pulses.

land on every surface. To test this theory two things were done; firstly the precipitant on the reaction chamber wall was analysed using FTIR. This was compared to the FTIR of each of the TGA steps of the different ratios studied. These show a strong resemblance to the product of the first weight loss step of calcium lactate ($3238\,cm^{-1}$, $1592\,cm^{-1}$, $1431\,cm^{-1}$, $1314\,cm^{-1}$, $1263\,cm^{-1}$, $1123\,cm^{-1}$, $1046\,cm^{-1}$, $932\,cm^{-1}$, $859\,cm^{-1}$, $774\,cm^{-1}$ and $666\,cm^{-1}$ for the precipitate versus $3268\,cm^{-1}$, $1590\,cm^{-1}$, $1431\,cm^{-1}$, $1314\,cm^{-1}$, $1263\,cm^{-1}$, $1124\,cm^{-1}$, $1043\,cm^{-1}$, $930\,cm^{-1}$, $860\,cm^{-1}$, $773\,cm^{-1}$ and $668\,cm^{-1}$ for calcium lactate). This implies that at the low temperature of the reaction chamber walls, the unreacted calcium lactate is dehydrating. Secondly, PP-MOCVD runs were performed at the ambient temperature with the same precursor as in the previous test. If the solution is not vapourising and decomposing the coating formed using ambient temperature will look the same as one using a deposition temperature.

The EDS results are in Table 6.9. SEM images were taken of a heated substrate and an unheated substrate, as shown in Figure 6.13. The heated substrates

	Deposition temperature	
Concentration	**Ambient**	**500°C**
0.150 mole%	64**Ca**:3**P**:341**O**:30**C**	4**Ca**:3**P**:20**O**:4**C**
0.075 mole%	70**Ca**:3**P**:358**O**:101**C**	5**Ca**:3**P**:24**O**:5**C**
0.009 mole%	C112**Ca**:3**P**:655**O**:19**C**	2**Ca**:3**P**:10**O**:4**C**

Table 6.9: Ratio of elements observed by EDS for ambient and heated runs.

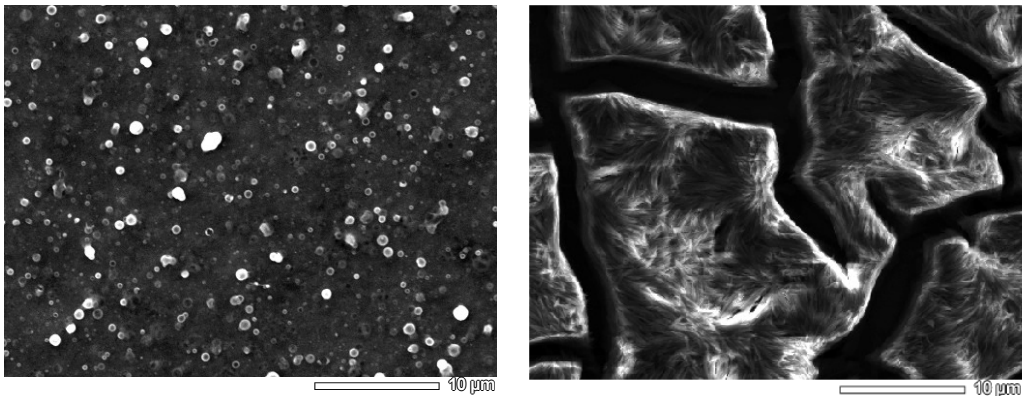

(a) (b)

Figure 6.13: SEM images of the 0.15 mole% precursor solution (a) with a deposition temperature of 500°C and (b) at ambient temperature.

developed a brown coating and the unheated developed a grey coating, which cracked and peeled off. From looking at the EDS, the SEM, the colour and the behaviour of the coatings, it is safe to say that the precursor solution is decomposing at or near the heated substrate and not just landing on the substrate.

6.7 Dried precursor solution

Another possible theory for why the surface is not uniform and a precipitate is forming, is that there are water molecules attached to the calcium lactate and in the methanol. These molecules could be evaporating and leaving a calcium lactate/TMP powder which is landing on the substrate and reactor walls. To test this theory the methanol was dried over $CaSO_4$, distilled and left over sieves during the PP-MOCVD run. The calcium lactate was dried in the kiln at 150°C, as this was the temperature at which the TGA study revealed that the attached water molecules evaporated off. This experiment was performed using different concentrations and their proportional number of pulses and compared to the experiments using wet precursors. The coatings formed were thin, as the nozzle was not spraying well. This also happened last time dry methanol was put through the PP-MOCVD. Thus the hypothesis could not be proved or disproved. However, putting dry methanol through the system does not appear to be a workable solution.

6.8 Conclusion

The precursor calcium lactate and TMP react with each other and form a calcium phosphate coating. An excess of TMP (5:24 or 5:30) is needed to form a coating with a calcium to phosphorus ratio similar to HAp. Annealing the substrate improves the element ratio; one or two hours is sufficient using either the 100 Pa pressure method or the atmospheric pressure method, as longer times do not significantly change the coating. If the temperature of annealing is too high most of the coating will disappear, leaving TiO_2. A temperature of 700°C was found to be the ideal annealing temperature as it resulted in a ratio of calcium to phosphorous the same as HAp and the surface was not entirely TiO_2. Annealing did not improve the coating attachment to the substrate as it still scratched off. Using a lower number of pulses (i.e., making a thinner coating) improved the ability of the coating to adhere. However, this still could be scratched off with tweezers.

Almost all of the coatings had carbon contaminants, which suggests that the coating being formed is a carbonated HAp or calcium carbonate formed from the decomposition of the calcium lactate which did not react with the TMP. Another possible reason why there is a large presence of carbon contaminants from PP-MOCVD compared to the TGA is the addition of methanol as the solvent. Using a higher deposition temperature improved the ratio of the calcium to phosphate and decreased the amount of carbon present, which suggests that the precursor is not decomposing entirely or the methanol is entirely evaporating. However, a better heating system would need to be designed to maintain the higher temperatures to fully test this theory.

None of the SEM images show uniform coatings with the ideal thickness. The reactor chamber was always coated in a white precipitate and attempts to fix this problem were unsuccessful. Changing the concentration of the precursor solution only caused the PP-MOCVD runs to take longer and using a dried precursor solution caused the nozzle to operate unsatisfactorily. The ambient tests did prove that the precursor was decomposing onto the substrate and not being deposited. Thus, there is hope that this precursor could still do what is desired.

Chapter 7

CONCLUSION

The goal of this research was to develop a bio-compatible coating for artificial bone implants. From looking at various coating precursors, calcium lactate was chosen as it is readily available commercially, is biologically friendly and has high solubility. The substrate used was titanium as the majority of bone implants are made from titanium.

Calcium lactate and TMP have been shown by the TGA and PP-MOCVD studies to react with each other to form a calcium phosphate compound. These tests also showed that an excess of TMP will give a compound that has a similar stoichiometry to HAp and not just tricalcium phosphate or dibasic calcium phosphate. The TGA proved that with an excess of TMP, the precursor decomposes at a lower temperature (400°C as opposed to 800°C). This implied that the deposition temperature required in the PP-MOCVD was at least 400°C. However, it was found that using a higher deposition temperature increased the likelihood of full decomposition.

The coatings formed by PP-MOCVD were shown by the SEM to be non-uniform. Annealing the coating did help with this and formed a coating with a closer

stoichiometry to HAp. However, if longer annealing times or higher annealing temperatures were used the coating degraded, leaving a TiO_2 substrate. A temperature of 700°C was the optimum annealing temperature and perhaps this would be a good deposition temperature for the PP-MOCVD. It is unknown why the coating was non-uniform, as the ambient PP-MOCVD run showed that the precursor was decomposing.

Most of the coatings contained carbon contaminants, which could have been due to unreacted calcium lactate or the formation of carbonated HAp. This may not be a problem in the overall scheme of the project, since natural bone contains trace amounts of carbonate. Having carbonate present may improve the bioactivity of the coating; this in turn could increase the strength, elasticity and durability of the coating.

7.1 Future work

There are several ways that future research could build on the results from this project. Changing the calcium precursor may form a more uniform coating of HAp at lower deposition temperatures. Extending the PP-MOCVD to work on three dimensional surfaces is required for practical use in bone replacements. The addition of trace elements or a phospholipid layer may improve the bone in-growth and extend the lifetime of the coatings.

7.1.1 Calcium precursor

Using a different calcium precursor, for example, calcium carbonate, calcium malate, calcium acetate or calcium oxalate, may result in a more uniform coating or decomposition at a lower temperature. A calcium precursor which contains no carbon, for example, $Ca(OH)_2$ or calcium oxide (CaO), would reduce the chance of carbon contamination. If there was still carbon present in the coating it would be from the TMP or the methanol solvent; this would give better insight into how the compounds react.

7.1.2 Substrate

The benefit of using PP-MOCVD is its ability to form uniform coatings on any shape. This needs to be verified using a porous substrate for improved mechanical lock of the implant to the bone. Another important feature is that bone implants are not flat and so the PP-MOCVD needs to be tested using three dimensional shapes, for example, titanium rods or screws. This area of expansion is being worked on currently by four mechanical engineering honours students at the University of Canterbury.

7.1.3 Trace elements

The closer the composition of the coating is to the composition of bone the more bioactive it is. Therefore the addition of trace metal and ionic compounds (e.g. Mg^{2+}, Fe^{2+}, CO_3^{2-}, F^-) to the precursor solution could result in a coating closer

to the composition of bone, increasing spontaneous bonding and integration with the bones involved. As with the calcium lactate and the TMP a full TGA study of the decomposition of these trace metals and the reaction with the HAp precursors would be required to find an appropriate ratio of trace metal to HAp. It is also important to do solubility tests on these new precursor mixtures to ensure that when they are put through the PP-MOCVD, they will not clog any of the tubing or the nozzle. Once this has been completed the new precursor solution would require testing in the PP-MOCVD at the optimum conditions to form HAp, as this is still the most important feature. The variables may need to be altered due to the way the trace metals react with the HAp precursors.

7.1.4 Phospholipid layer

Adding a phospholipid phosphatidylserine layer to the coating could enhance the osteoblast activity, promote mineralization and facilitate bone in-growth. Osteoblasts are mono-nucleate cells which are responsible for bone formation and they control the rate of mineralization by secretion of vesicles that have a phospholipid bi-layer. This bi-layer is the primary site of HAp nucleation and mineralization. The dual-layer of HAp and phosphatidylserine will lead to faster bone in-growth, can be used to reduce blood clot risks by filling the space between implant surface and bone, and can be loaded with drugs for local delivery of antibiotics or cancer therapeutics. Characterization of dual-layer coated implant surfaces for *in vitro* bio-mineralization potential, using simulated body fluid and carboplatin pharmacokinetics using elution studies, would need to be performed.

Due to the price of phosphatidylserine, phosphatidylcholine could be used as a model phospholipid. This will require testing in the PP-MOCVD apparatus to find how well it sprays and the deposition temperature needed for it to attach to the HAp coating without decomposing, as if it decomposes it will lose its usefulness.

Appendix A

PP-MOCVD APPARATUS COMPONENTS

The PP-MOCVD apparatus consists of four main components, as shown in Figure A.1. They are the precursor supply system, the ultrasonic atomization system, the reaction chamber and the exhaust system.

A.1 Precursor supply system

With each pulse the precursor supply system delivers a measured volume of the liquid precursor to the reactor chamber. This is achieved by pressurizing the precursor and purge bottles with argon gas; the supply pressure is controlled by a gas pressure regulator and monitored using a pressure gauge. The precursor and purged liquid will then flow out of the pressurised pyrex bottles and into the delivery tubes attached. These tubes are connected to a three way valve; the available positions are precursor on, purge on and off. The chosen position controls which liquid will be drawn into valve 1 (V1) of the valve system. This system only uses four ports of a six port external sample injector to pulse the liquid into the reactor chamber. In this system there are two positions shown by

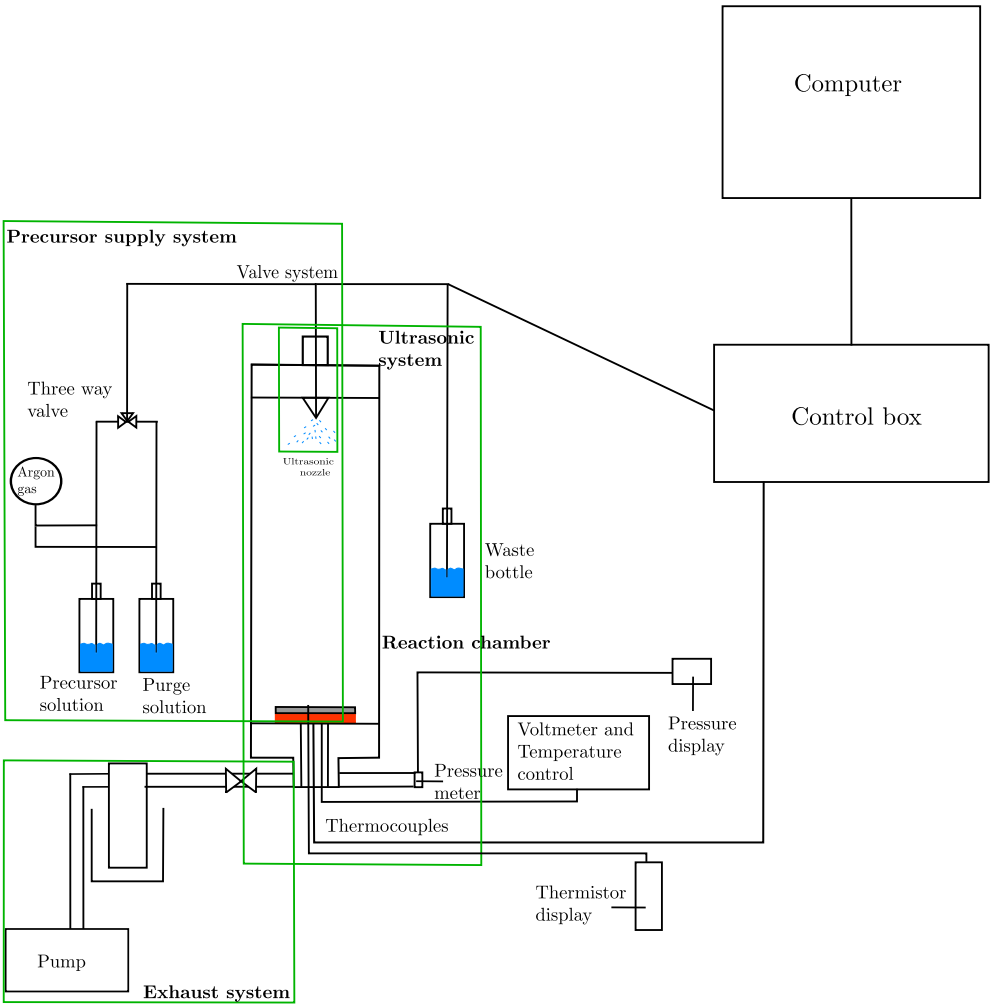

Figure A.1: Diagram of PP-MOCVD.

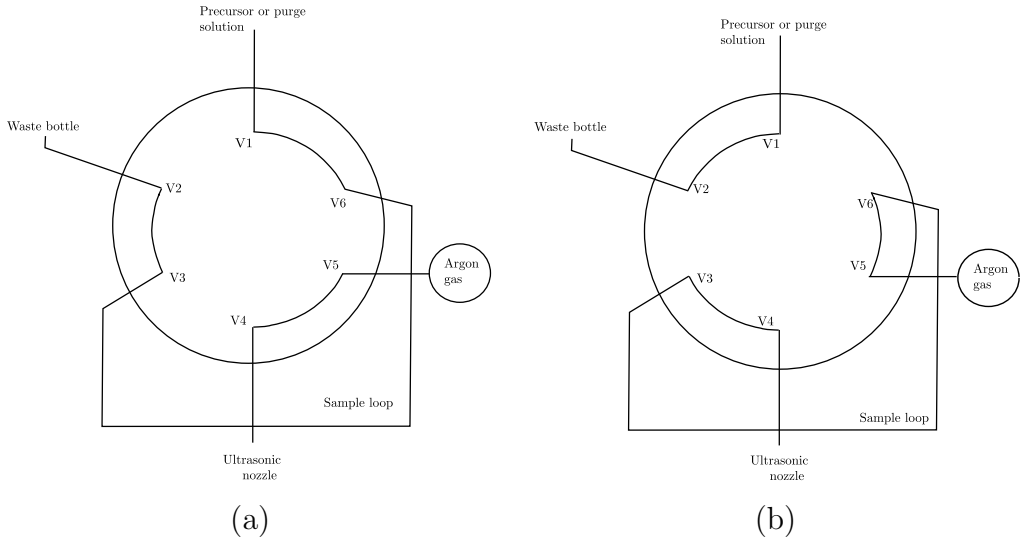

Figure A.2: Valve positions (a) A and (b) B.

Figure A.2. When it is set in position A, V1 and valve 3 (V3) are open, and valve 2 (V2) and valve 4 (V4) are closed. The opposite is true in position B; in both positions valve 5 (V5) and valve 6 (V6) are open. In position A the liquid will flow through V1 and V6 to fill the sample loop. This gives the desired volume of liquid; any surplus liquid flows out through V3 to be vented out as waste when V2 is open. Once the liquid has flowed through, V3 closes followed by V1 and then V4 and V2 open (position B). In this position a shot of argon enters through V4, proceeds to V3 and displaces the liquid in the sample loop through V6 and V5 into the ultrasonic atomisation nozzle. Any waste liquid is removed through V2. After a set time V2 closes followed by V4 and then it is moved back into position A. These pulses are controlled using a LabView program; this also gives a digital display of the pressure variation over time, as shown in Figure A.3.

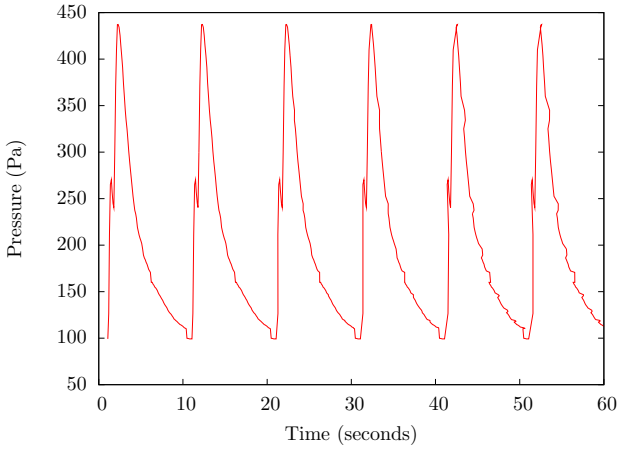

Figure A.3: A representation of the pulse pressure flow cycles.

A.1.1 Solutions

There are two solutions needed in the precursor supply system. The first is the precursor; this was prepared by dissolving varying amounts of calcium lactate with varying volumes of trimethyl phosphate in 200 mL of methanol. This is placed in a pyrex supply bottle which is well sealed and has a custom made lid. The other solution is the purge solution, which is propanol; this is used to flush out the tubes and ultrasonic atomisation nozzle after each experiment.

A.2 Ultrasonic atomisation nozzle

The ultrasonic atomisation nozzle used was manufactured by SONO-TEK. It consists of a nozzle which is connected to the tubing from V5 and a broadband ultrasonic generator. This nozzle was used to assist the vaporisation of the precursor molecules by atomising the precursor liquid. To achieve this the liquid

is exposed to ultrasound waves (sound waves of higher frequency than audible sound waves). This creates ultrasonic vibrations within the liquid, which disrupts the surface tension of the liquid, thus creating holes where there is no surface tension. The liquid can then escape through these holes producing droplets with a diameter of about 15 μm. All depositions were performed at the SONO-TEK suggested upper power limit of 5.0W.

A.3 Reaction chamber

The reaction chamber is a pyrex cylinder with a diameter of 105 mm and height of 350 mm, as seen in Figure A.4. The glass tube of the chamber is screwed into the base and the top of the reactor chamber. These must be tight so the O-rings on either end are compressed to form a vacuum seal. The nozzle is mounted in the middle of the reactor top. The heater and reaction surface sit at the bottom of the reaction chamber. The base of the chamber has inlets for the vacuum pump and air, as well as connections to the pressure gauge, the thermocouple display and the voltage meter.

The heater was manufactured in-house and the heater consists of a coiled kanthal wire which is set in clay. The reaction surface is placed over the heater; this surface is where the substrates are placed and is polished between experiments to remove any contamination. The heater is placed within a holder which serves as a heat shield and another layer of metal is wrapped around the holder as extra protection. There are two K-type thermocouples within the chamber; one measures the temperature inside the heater and the other measures the temperature

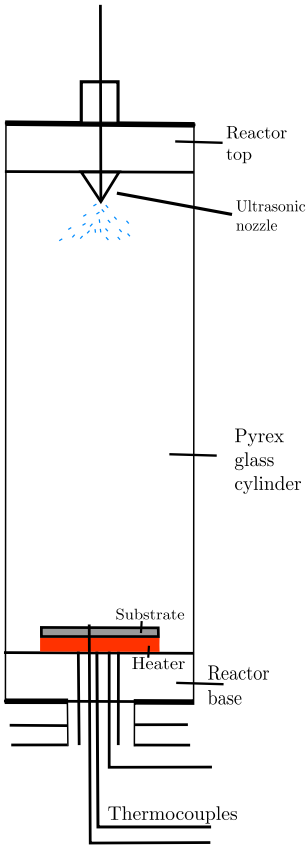

Figure A.4: Diagram of PP-MOCVD reactor chamber.

on top of the surface.

A.4 Exhaust system

This setup uses a Varian SD-200 oil mist trap pump to provide the vacuum. Between the pump and the reactor chamber is a butterfly valve, which controls the vacuum pressure in the reactor and a valve that opens up to the air to remove the vacuum so the chamber can be opened. Once the liquid has been pulsed into the reactor chamber, the exhaust goes through a liquid nitrogen trap which

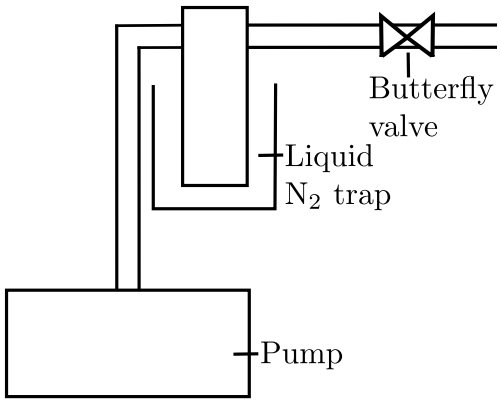

Figure A.5: Diagram of PP-MOCVD exhaust system.

condenses any chemicals, as shown in Figure A.5, thus protecting the pump.

Appendix B

OPERATION OF PP-MOCVD

To increase repeatability of experiments and to minimize the errors the following procedure was followed for all experiments.

B.1 Precursor preparation

The concentration of the precursor solution for each experiment was calculated with the following equation:

$$C_{\text{mol\%}} = \frac{n_{\text{Calcium precursor}}}{n_{\text{Calcium precursor}} + n_{\text{solvent}}} \tag{B.1}$$

B.2 Substrate preparation

- Wash substrate with detergent and then cover with acetone.
- Place in the ultrasonic water bath for 3 min.
- Rinse with ethanol and dry with air.

B.3 Surface preparation

- Rinse surface with ethanol and dry with air.
- Place on top of the heater.
- Screw base column in and insert into cylinder holder.
- Thermocouple one is inserted under the surface.
- The heater wires are screwed into the bus.
- Thermocouple two is pegged to the surface.
- The substrate is pegged to the surface by the edges.
- Wrap insulation coat around the heater.

B.4 Reactor preparation

- Clean glass cylinder with ethanol and dry with air.
- Put rubber ring on either end and screw cylinder in place.

B.5 Precursor preparation

- Prepare precursor in a precursor bottle.
- Install in system.
- Put loose end in waste bottle.

B.6 Equipment set up

- Turn on pressure meter, control box, voltmeter and thermocouple display.
- Turn air inlet valve off.
- Turn vacuum pump valve on.
- Put liquid nitrogen into flask and position gas trap in it.
- Turn on fume hood.
- Turn on pump.

B.7 Variables set up

- Change voltage to increase the temperature in the reactor.
- Once heated to desired temperature leave for 30 min to purge impurities.
- Turn on argon and set to 70kPa.
- Turn on air pressure to 280kPa.

B.8 Experimental start up

- Turn precursor valve on; if argon pressure drops, turn off and check for leaks.
- Turn off precursor valve.

- Turn purge bottle valve on.
- Turn the three way to purge on.
- Switch controls to manual.
- Switch V3 on.
- Switch V1 on.
- If waste is going into the waste bottle there are no clogs.
- Switch V1 off.
- Switch V3 off.
- Switch controls to automatic.
- Turn the three way valve to off.
- Turn the purge bottle valve off.
- Turn the precursor valve on.
- Turn the three way valve to precursor on.
- Switch to manual.
- Switch V3 on.
- Switch V1 on.
- Make sure there are no clogs by checking the waste is going into the waste bottle.
- Switch V1 off when the injection line has filled up with precursor.

- Switch V3 off.
- Switch controls to automatic.
- Adjust air bleed until the pressure is 100Pa.

B.9 Computer setup

- Open My Computer.
- Open Local Disk (C:).
- Open users.
- Open NewCVD.
- Open Pulsed_ CVD4.vi.
- Change any variable on screen as desired (e.g. number of cycles and filling time).
- Press the white arrow at the top left hand side.
- Double click on Save Data (until it glows green).
- Turn on ultrasonic nozzle.
- Press start.
- Regularly check the precursor temperature.

B.10 Shutdown

- Press stop (if wanting to stop before the set number of cycles).
- Turn off ultrasonic nozzle.
- Set number of cycles to 20.
- Turn the three way valve off.
- Turn the precursor valve off.
- Turn the three way valve to purge on.
- Turn purge bottle valve on.
- Switch controls to manual.
- Switch V3 on.
- Switch V1 on.
- If waste is going into the waste bottle there are no clogs.
- Switch V1 off.
- Switch V3 off.
- Switch controls to automatic.
- Turn on ultrasonic nozzle.
- Press start on screen.
- Let it run in order to clean nozzle and injection lines.

- Once stopped turn off ultrasonic nozzle.
- Switch controls to manual.
- Switch V3 on.
- Switch V1 on.
- If waste is going into the waste bottle there are no clogs.
- Switch V1 off.
- Switch V3 off.
- Switch controls to automatic.
- Turn off air pressure and argon (gauge and bottle).
- Close air bleed.
- Turn heater down slowly in order no to crack the film.
- Turn off control box and pressure meter.
- Maintain under vacuum while cooling down for 2hrs.
- Close vacuum pump valve.
- Turn off pump.
- Open air inlet valve.
- Remove liquid nitrogen flask.
- Remove precursor from system and store away from light in a desiccator.
- Turn off fume hood.

Appendix C

ABBREVIATIONS

APCVD Atmospheric Pressure Chemical Vapour Deposition

calcium acetylacetone bis(2,4-dioxopentan-3-ido)calcium

$CaCl_2$ calcium chloride

calcium benzoylacetone bis(1-phenyl-1,3-dioxobutan-2-ido)calcium

calcium dibenzoylmethane bis(1,3-diphenyl-1,3-dioxopropan-2-ido)calcium

CaO calcium oxide

$Ca(OH)_2$ calcium hydroxide

CVD Chemical Vapour Deposition

dbm dibenzoyl methane

EDS Energy Dispersive Spectroscopy

FTIR Fourier Transform Infra-Red spectroscopy

HAp hydroxyapatite

HVOF High Velocity Oxy-Fuel

LECVD Laser Enhanced Chemical Vapour Deposition

LPCVD Low Pressure Chemical Vapour Deposition

MBE Molecular Beam Epitaxy

MOCVD Metal-Organic Chemical Vapour Deposition

PECVD Plasma Enhanced Chemical Vapour Deposition

PMMA polymethylmethacrylate

PP-MOCVD Pulse Pressure Metal-Organic Chemical Vapour Deposition

PVD Physical Vapour Deposition

SEM Scanning Electron Microscope

TiO_2 titanium dioxide

TGA Thermogravimetric Analysis

TMP trimethyl phosphate

UHVCVD Ultra-High Vacuum Chemical Vapour Deposition

UV ultra-violet

REFERENCES

[1] Carpenito-Moyet, L. J. *Nursing Care Plans and Documentation: Nursing Diagnosis and Collaborative Problems*; Lippincott Williams and Wilkins, 2008.

[2] Perry, C. R.; Court-Brown, C. M. *Mastercases: Orthopaedic Trauma*; Thieme, 1999.

[3] Amin, A. K.; Sales, J. D.; Brenkel, I. J. *Current Orthopaedics* **2006**, *20*, 216–221.

[4] Wendelboe, A.; Hegmann, K.; Briggs, J.; Cox, C.; Portmann, A.; Gildea, J.; Gren, L.; Lyon, J. *American Journal of Preventive Medicine* **2003**, *25*, 290–295.

[5] Campbell, A. A.; Fryxell, G. E.; Linehan, J. C.; Graff, G. L. *Journal of Biomedical Materials Research* **1996**, *32*, 111–118.

[6] Schlossberg, L.; Zuidema, G. D.; Johns Hopkins University. School of Medicine, *The Johns Hopkins Atlas of Human Functional Anatomy*; JHU Press, 2004.

[7] Katta, J.; Jin, Z.; Ingham, E.; Fisher, J. *Medical Engineering and Physics* **2008**, *30*, 1349–1363.

[8] Sun, L.; Berndt, C. C.; Gross, K. A.; Kucuk, A. *Journal of Biomedical Materials Research* **2001**, *58*, 570–592.

[9] Koch, C.; Johnson, S.; Kumar, D.; Jelinek, M.; Chrisey, D.; Doraiswamy, A.; Jin, C.; Narayan, R.; Mihailescu, I. *Materials Science and Engineering: C* **2007**, *27*, 484–494.

[10] Haynes, D. R.; Crotti, T. N.; Zreiqat, H. *Biomaterials* **2004**, *25*, 4877–4885.

[11] Futani, H.; Minamizaki, T.; Nishimoto, Y.; Abe, S.; Yabe, H.; Ueda, T. *The Journal of Bone and Joint Surgery, Incorporated* **2006**, *88*, 595–603.

[12] Hosalka, H. S.; Dormans, J. P. *Pediatric Blood Cancer* **2004**, *42*, 295–310.

[13] Shin, D.; Choong, P. F.; Chao, E. Y. H.; Sim, F. H. *Acta Orthopaedica Scandinavica* **2000**, 302–311.

[14] Miyamoto, Y.; Kaysser, W. A.; Rabin, B. H. *Functionally Graded Materials*; Springer, 1999.

[15] Davis, J. R.; ASM International, *Handbook of Materials for Medical Devices*; ASM International, 2003.

[16] Buchanan, R. A.; Rigney, E. D.; Griffin, C. D. *American Society for Testing and Materials Special Technical Publication* **1987**, 105–114.

[17] Turek, S. *Orthopaedics: Principles and Applications*; J.B Lippincott, 1984.

[18] Okazaki, M. *Phosphorous Research Bulletin* **2004**, *17*, 1–8.

[19] Epinette, J.-A.; Manley, M. T. *Fifteen Years of Clinical Experience with Hydroxyapatite Coatings in Joint Arthroplasty*; Springer, 2004.

[20] Pierson, H. O. *Handbook of Chemical Vapor Deposition (CVD) : Principles, Technology, and Applications (2nd edition)*; Noyes Publications, 1999.

[21] Cave, H. M.; Krumdieck, S. P.; Jermy, M. C. *Chemical Engineering Journal* **2008**, *135*, 120–128.

[22] Mattox, D. M. *Handbook of Physical Vapor Deposition (PVD) Processing: Film Formation, Adhesion, Surface Preparation and Contamination Control*; William Andrew Inc., 1998.

[23] Franssila, S. *Introduction to Microfabrication*; John Wiley and Sons, 2004.

[24] Davis, J. R.; J.R. Davis and Associates,; ASM International Thermal Spray Society Training Committee, *Handbook of Thermal Spray Technology*; ASM International, 2004.

[25] American Society for Metals,; ASM International Handbook Committee,; ASM International Alloy Phase Diagram Committee, *ASM Handbook*; ASM International, 1990.

[26] Wang, Z. L.; Liu, Y.; Zhang, Z. *Handbook of Nanophase and Nanostructured Materials: Materials Systems and Applications I*; Springer, 2003.

[27] Suryanarayanan, R. *Plasma Spraying: Theory and applications*; World Scientific, 1993.

[28] Todd, R. H.; Allen, D. K.; Alting, L. *Fundamental Principles of Manufacturing Processes*; Industrial Press Inc, 1994.

[29] Lee, S.; Lee, L. *Encyclopedia of Chemical Processing*; CRC Press, 2005.

[30] Tuller, H. L.; Schoonman, J.; Riess, I. *Oxygen Ion and Mixed Conductors and their Technological Applications*; Springer, 2000.

[31] Goyal, A. *Second-generation HTS Conductors*; Springer, 2005.

[32] Rahaman, M. N. *Ceramic Processing and Sintering*; CRC Press, 2003.

[33] *Handbook of Thin-Film Deposition Processes and Techniques : Principles, Methods, Equipment and Applications*; Seshan, K., Ed.; Noyes Publications/William Andrew Pub, 2002.

[34] Bunshah, R. F. *Handbook of Deposition Technologies for Films and Coatings: Science, Technology, and Applications*; William Andrew Inc., 1994.

[35] Baluti, S. I. M.Sc. thesis, Mechanical engineering at the University of Canterbury, Christchurch, New Zealand, 2005.

[36] Saddow, S. E.; Agarwal, A. *Advances in Silicon Carbide Processing and Applications*; Artech House, 2004.

[37] Hull, R.; Bean, J. C. *Germanium Silicon: Physics and Materials*; Academic Press, 1998.

[38] Zant, P. V. *Microchip Fabrication: A Practical Guide to Semiconductor Processing*; McGraw-Hill Professional, 2004.

[39] Ohring, M. *Materials Science of Thin Films: Deposition and Structure*; Academic Press, 2002.

[40] El-Kareh, B. *Fundamentals of Semiconductor Processing Technology*; Springer, 1995.

[41] Hocking, M. G.; Vasantasree, V.; Sidky, P. *Metallic and Ceramic Coatings : Production, High Temperature Properties, and Applications*; Longman Scientific and Technical, 1989.

[42] Rodriguez, J. A.; Garcia, M. F. *Synthesis, Properties, and Applications of Oxide Nanomaterials*; Wiley-Interscience, 2007.

[43] Siriwongrungson, V.; Alkaisi, M. M.; Krumdieck, S. P. *Surface and coatings technology* **2007**, *71*, 8944–8949.

[44] Kristinsdottir, A. M.Sc. thesis, Mechanical Engineering at the University of Canterbury, Christchurch, New Zealand, 2006.

[45] Krumdieck, S. Ph.D. thesis, Mechanical Engineering at the University of Colorado, Boulder, United States of America, 1999.

[46] Krumdieck, S. P.; Sbaizero, O.; Bullert, A.; Raj, R. *Journal of the American Ceramic Society* **2002**, *85*, 2873–75.

[47] Krumdieck, S. P.; Sbaizero, O.; Bullert, A.; Raj, R. *Surface and Coatings Technology* **2003**, *167*, 226–233.

[48] Sukul, N. C. *High Dilution Effects: Physical and Biochemical Basis*; Springer, 2004.

[49] Stachowiak, G. *Experimental Methods in Tribology*; Elsevier, 2004.

[50] Orton, *Thermal Gravimetric Analysis*.

[51] Olmsted, J.; Williams, G. M. *Chemistry: the Molecular Science*; Jones and Bartlett Publishers, 1996.

[52] Schwoeble, A. J.; Exline, D. L. *Current Methods in Forensic Gunshot Residue Analysis*; CRC Press, 2000.

[53] Luckey, H. A.; Kubli, F.; Committee F-4 on Medical and Surgical Materials and Devices,; ASTM Committee B-10 on Reactive and Refractory Metals and Alloys, *Titanium Alloys in Surgical Implants: a Symposium*; ASTM International, 1983.

[54] Krumdieck, S. P.; Kristinsdottir, A.; Ramirez, L.; Lebedev, M.; Long, N. *Surface and Coatings Technology* **2007**, *201*, 8908–8913.

[55] Allen, G.; Ciliberto, E.; Fragal, I.; Spoto, G. *Nuclear Instruments and Methods in Physics Research B* **1996**, *116*, 457–460.

[56] Darr, J. A.; Guo, Z. X.; Raman, V.; Bououdina, M.; Rehman, I. U. *Chemical Communication* **2004**, *6*, 696–697.

[57] Hartshorn, R.; Stockwell, S.; Lebedev, M.; Krumdieck, S. *Surface and Coatings Technology* **2007**, *201*, 9413–9416.

[58] Stockwell, S. C. BSc(Hons) project report, University of Canterbury, Christchurch, New Zealand.

[59] Sigma-Aldrich Corporation, *Aldrich Advancing Science*; Sigma-Aldrich corporation, 2005.

[60] Hamdia, M.; Ektessabi, A. *Surface and Coatings Technology* **2006**, *201*, 3123–3128.

[61] Ding, S.; Huang, T.; Kao, C. *Surface and Coatings Technology* **2003**, *165*, 248–257.

[62] Boyd, A. R.; Burke, G. A.; Duffy, H.; Cairns, M. L.; O'Hare, P.; Meenan, B. J. *Journal of Materials Science-Materials in Medicine* **2008**, *19*, 485–498.